



**UCGE Reports
Number 20220**

Department of Geomatics Engineering

**Change Detection of Man-made Objects Using Very
High Resolution Images**

(URL: <http://www.geomatics.ucalgary.ca/links/GradTheses.html>)

by

Santosh Phalke

May 2005



**UNIVERSITY OF
CALGARY**

Abstract

Most of the research in remote sensing is focused on developing well-defined and reliable automated processes for the extraction of information from different types of imagery. In this communication, we are dealing with the extraction of linear man-made objects (especially buildings) in urban areas and the determination of changes in these objects using very high resolution IKONOS imagery. The modern world needs accurate information about these changes for urban planning and Geospatial Information Systems updating.

Newly developed change detection approach is based on feature extraction using interesting points and edges. Linear rectangular features such as buildings can be defined by corner points and edges joining those corner points. The features have been extracted using different types of edge detectors and the Forstner corner detector (Forstner, 1994).

In order to discriminate linear man-made objects from other man-made objects (such as roads), it is necessary to link the corners and their corresponding edges for each linear man-made object. For each corner point, the direction of gradient of the edges is determined by matching them to an 'L' shape template. A line following method is then applied to determine all the edges between the corner points. We have found that each man-made object formed different groups of corner points and edges, which is useful to classify them as a separate individual object.

Furthermore the developed 'L' shape template matching method has also been implemented on the Blue band of the pan-sharpened image obtained using Ikonos multispectral and panchromatic images. The comparison of the developed method results

obtained using Blue pan-sharpened band has been carried and shown that Blue band provides better results when compared with panchromatic-based results.

To detect changes in man-made objects between the 2001 and 2002 IKONOS images, the same man-made objects (*i.e.* large buildings) have been extracted in both images. Using positional information and feature matching techniques the changes have been determined. For the validation and improvement of the results, changes obtained using newly developed technique is compared with changes obtained from a Principle Component Analysis (PCA) method (Singh, 1989) and from a supervised classification method (Howarth *et al.*, 1981). This comparison demonstrated that the new developed method provided better results.

Preface

This is an unaltered version of the author's Master of Science thesis of the same title. The Faculty of Graduate Studies accepted this thesis in May 2005. The faculty supervisor of this work was Dr. Isabelle Couloigner, and the other members of the examining committee were Dr. Ayman Habib and Dr. Darren Bender.

Acknowledgement

Many persons and organisations contributed to this thesis work. I would like to express my gratitude especially

- To the two pillars of my life, my mother and lovely wife, for their love and support throughout the work
- To Dr. Isabelle Couloigner, my supervisor for her unconditional support, help and supervision through all the phases of my M Sc program
- To Dr. Ayman Habib, for sharing his expertise with me, and guiding me the right direction of research
- To Mr. Qiaoping Zhang, for support and guidance throughout the course of my M Sc work
- To all my colleagues in Information and Land Tenure Lab, for a nice environment during this research
- To “Geoide”, for providing the financial support for this project work
- To the City of Fredericton, for providing the valuable IKONOS dataset
- To, the University of Calgary, for providing URN dataset

Table of Contents

Abstract.....	i
Preface.....	iii
Table of Contents	v
List of Tables	vii
List of Figures	viii
List of Symbols	x
CHAPTER 1	1
1.1 Background	1
1.2 Research Objectives.....	8
1.3 Thesis Organization.....	8
CHAPTER 2	10
2.1 Background.....	10
2.2 Challenges.....	11
2.3 Change Detection Methods.....	14
2.3.1 Image to Image Change Detection.....	15
2.3.2 Image to Site Model Change Detection.....	20
2.3.3 Image to GIS Change Detection	22
2.4 Conclusion	23
3.1 Introduction.....	26
3.2 Low Level Feature Extraction.....	27
3.2.1 Principle Component Analysis Method for Image Fusion.....	29
3.2.2 Intensity Hue Saturation (IHS)	30
3.2.3 High Pass Filter.....	30
3.3 Medium and High Level Feature Extraction.....	30
3.3.1 Edge-based Segmentation.....	31
3.3.2 Edge Detection.....	31
3.3.3 Edge Detection Using First Order Derivatives	33
3.3.4 Edge Detection Using Second Order Derivative	34
3.3.5 Comparison of First and Second Order Derivative Operators.....	35
3.4 Corner and Interesting Point Feature Detection.....	35
3.4.1 Moravec Interest Operator	38
3.4.2 Harris/Plessey Corner Detector	39
3.4.3 Smallest Univalued Segment Assimilating Nucleus (SUSAN) Corner Detector.....	40
3.4.4 Forstner Corner Detector	41
3.5 Conclusion	45
CHAPTER 4	46
4.1 Preliminary Change Detection.....	46
4.2 Data Set Used.....	47

4.3	Pre-Processing Steps.....	47
4.4	Principle Component Analysis.....	49
4.4.1	Data Set Used.....	51
4.4.2	Implementation of Image to Image Change Detection using PCA.....	51
4.4.3	Analysis of the Results Obtained Using PCA Technique.....	56
4.4.4	Implementation of Image to GIS Change Detection using Post Classification Change Detection.....	57
4.4.5	Change Detection of Buildings.....	61
4.5	Limitations of the Traditional Change Detection Method.....	62
5.1	Introduction.....	64
5.2	Need for the Feature Extraction Based Technique.....	65
5.3	Frame Work for the ‘L’ Shape Template Matching Automated Building Extraction Technique.....	66
5.3.1	Geo-Referencing and Image Enhancement.....	67
5.3.2	Edge Detection.....	67
5.3.3	Linear Feature Extraction.....	68
5.3.4	Curvilinear Feature Extraction.....	71
5.3.5	Identification of the Extracted Objects.....	72
5.3.6	Listing of the Extracted Objects.....	72
5.4	Results of Change Detection Based On Automated Building Extraction Process.....	73
5.5	Implementation of the ‘L’ Shape Template Matching Method on the Blue Band of the Fused Image.....	78
5.5.1	Analysis of the Derived Change using the Pan-sharpened Blue Band.....	84
5.6	Requirements for the ‘L’ Shape Template Matching Technique.....	84
5.7	Observations.....	84
6.1	Qualitative Comparison of the Implemented Methods.....	86
6.1.1	Change Detection using Supervised Classification.....	86
6.1.2	Change Detection using PCA.....	87
6.1.3	Change Detection using ‘L’ Shape Template Matching.....	87
6.2	Quantitative Comparison.....	88
6.3	Summary.....	91
CHAPTER 7.....		92
References.....		94

List of Tables

Table 4.1 Classification accuracy of the classified image derived from the supervised classification.....	61
Table 6.1 Quantitative comparison of the implemented change detection techniques	89

List of Figures

Figure 3.1 Example of misclassification.....	28
Figure 3.2 (a) Gray level variations along the edge and its effect on detected edges (b) Example showing effect of gray level variation on detected edges	32
Figure 3.3 First and second derivatives of a function (a) Represents first derivative of the edge (b) the second derivative of the edge	33
Figure 3.4 Gray level variations around the interesting point.....	37
Figure 3.5 Corner detection using circular SUSAN kernel (Smith and Brady, 1997).....	40
Figure 3.6 Model for estimating corners and center of the circular symmetric feature (Forstner, 1994) (a) The edge element through (r_i, c_i) is represented by a straight line (l_i, Φ_i) . (b) The slop element through (r_i, c_i) is represented by the straight line $(l_i, \Phi_i$ $\bullet)$	42
Figure 4.1(a) Subset of Ikonos 2001 Image, (b) Enhanced subset of the Ikonos 2001 Image.....	49
Figure 4.2 Change detection using PCA transformation (Wiemker <i>et al.</i> , 1997).....	50
Figure 4.3 Change detection using PCA technique (Case Study 1).....	52
Figure 4.4 Change detection using PCA technique (Case Study Two)	53
Figure 4.5 Parameter space plot obtained (case study 1 and 2) after the PCA transformation.....	55
Figure 4.6 (a) Multispectral Ikonos image (b) Training data set used for the classification	58
Figure 4.7 (a) Classified Image obtained using supervised classification, (b) Assigned (pseudo) colour schema for the classified image	60

Figure 4.8 (a) Building layer of NTDB data set, (b) Derived building layer using classification (c) Derived change between GIS building layer and classified image building layer using PCA technique	62
Figure 5.1 Frame work for the Building extraction	66
Figure 5.2 Corner point detection using ‘L’ shape template matching.....	69
Figure 5.3 Missing pixels in the object.....	70
Figure 5.4 Example of semi-curvilinear feature	72
Figure 5.5 Input images used for extraction of buildings	73
Figure 5.6 Second stage input images to obtain modified object boundaries.....	75
Figure 5.7 Final results of the automated building extraction process	77
Figure 5.8 Pan-sharpening via the IHS technique.....	79
Figure 5.9 Input images used for extraction of buildings using Blue band of fused images obtained using IHS technique	81
Figure 5.10 Second stage input images to obtain modified object boundaries for change detection of man-made object using the blue band of the fused images.....	82
Figure 5.11 Final results of the automated building extraction process using the blue band of the fused images	83
Figure 6.1 Digitized reference images for change detection	90

List of Symbols

Σ	Summation
θ	Theta
μ	Micro
σ	Standard Deviation
$\sqrt{\quad}$	Square root
C_i	Covariance
$^\circ$	Degrees
O	Weighted Sum
W_i	Weight
∇	Gradient

List of Abbreviations

2-D	Two Dimensional
3-D	Three Dimensional
BDT	Background Discriminant Transformation
CV	Computer Vision
DSM	Digital Surface Model
IFOV	Instantaneous Field of View
GIS	Geospatial Information Systems
HPF	High-Pass-Filter
IFSAR	Interferometric Synthetic Aperture Radar
IHS	Intensity Hue Saturation
Laser	Light Amplification by Stimulated Emission of Radiation
LIDAR	LIght Detection and Ranging
PC	Principle Component
PCA	Principal Component Analysis
PCT	Principal Components Transformation
PC	Principle Component
PC1	Principle Component One
PC2	Principle Component Two
RGB	Red, Green, and Blue
SAR	Synthetic Aperture Radar
SUSAN	Smallest Univalued Segment Assimilating Nucleus
VHR	Very High Resolution

Chapter 1

Introduction

1.1 Background

Change detection is a process of identifying differences in the state of object or phenomena by observing them at different times (Singh, 1986). This thesis deals with the extraction of man-made objects (especially buildings) in urban areas and the determination of changes in these objects using very high resolution IKONOS imagery. The modern world needs accurate information about these changes for updating Geospatial Information Systems (GIS) and databases. The updated GIS information is utilized for important applications such as: city planning, industrial planning, road networking, property evaluation, disaster management and so on.

The process of change detection of man-made objects consists of three major steps: image registration, feature (object of interest) extraction and detection of geometric differences in the extracted features from the temporal images of the same location. Various techniques are available for precise image registration. This research used orthorectified IKONOS images for the change detection. Accurate extraction of man-made objects such as buildings is possible due to the availability of Very High Resolution (VHR) images. Remotely sensing images with less than 2 metre spatial resolution are recognized as very high resolution images (Gautama and Goeman, 2004). The extracted objects from VHR temporal image sets are then compared to detect the changes. Thus

change detection of man-made objects depends completely on the extraction of the objects of interest.

The extraction of man-made objects located in heterogeneous urban areas is a very difficult task due to the presence of different types of objects such as trees, large size containers, roads, parking lots. To discriminate the object of interest from the other objects, a pre-processing of the temporal images is necessary. This pre-processing can be based on image classification utilizing the spectral response property of each of the objects. For example, spectral reflectance of vegetation is high in the region of 0.75-1.35 μm and spectral reflectance of rocks and construction material used for the buildings is high in the region range of 2.0-2.5 μm . Hence it is possible to discriminate buildings from the vegetation based on the spectral reflectance property.

Most of the research in remote sensing is focused on developing well-defined and reliable automated processes for the extraction of geospatial information from different types of imagery (Hinz and Baumgartner, 2003). Recent advancement of sophisticated imaging acquisition techniques has made large and very high resolution data available for remote sensing research (Gautama and Goeman, 2004). Computer Vision (CV) enables researcher to extract features of interest. It uses accurate geospatial information such as location, size, shape, elevation, type of the objects for the extraction of the features. The primary goal of CV is to reconstruct the three dimensional (3-D) world from two dimensional (2-D) images and to interpret and describe it in a useful manner (Schenk, 1999). Several fundamental problems make the development of CV system difficult and limit their applications. The digital images may contain not only a lot of unneeded, but also misleading data such as shadows, occlusion effects, relief displacement effects,

cloud coverage. The basic tasks of CV are making information explicit, designing reasonable representations and describing objects in a form that is independent of the different illumination and viewpoint conditions like for example in GIS data sets (Schenk, 1999). One of the simple techniques for elimination of the difference due to the viewpoint and illumination condition is to define the object of interest using edges and interesting points (corner points of the features) (Mirmehdi *et al.*, 1996; 1998). This eliminates differences by conversion of the raster format into the vector format.

In general, change detection is used for environmental monitoring and agricultural applications. Land-use and land-cover changes are important for environmental studies (Fischer, 1995). Natural events such as weather, flooding, fire, climate fluctuation and ecosystem dynamics are responsible for changes in land-cover. Land-cover is also altered by direct human activities such as agricultural, encroachment of forest, urban construction and development, fuel consumption, and so on (NRC, 2001).

Change detection of man made objects using satellite remote sensing images has many applications such as urban planning, property evaluation, disaster management, urban sprawl and road network mapping (Wiggins *et al.*, 2000). Change detection of man-made objects gives information about newly constructed buildings, parks, roads that is useful for determining approximate increase in population or industrial area. This information is useful to determine needs of new parking lots, malls or schools for an urban area (Jensen *et al.*, 2004). The value of a property is based on its size and location. In other words the value of a property is largely dependent on its connectivity to road network, shopping complex, schools, offices, and so on (Boarnet and Chalermpong, 2002). Change detection of man-made objects can implicitly provide this information for

property evaluation. Earthquake, volcanoes, cyclones and tsunami cause huge damage and destroy man-made objects such as houses, buildings, roads or bridges. One can plan more accurately the rescue operation using the derived change information of man-made objects. Urban sprawl determines the direction and rate of a city growth and is also based on change detection (Anthony and Xia, 1999).

Different approaches have been adopted by researchers for change detection based on the details of the information needed (Shettigara *et al.*, 1995). These approaches can be categorized in three groups. The first approach is a preliminary change detection using optical remote sensing. The second approach deals with microwave remote sensing. The third approach is based on the image to geometrical model based change detection which is also known as 'Change Analysis' (Shettigara *et al.*, 1995).

Supervised classification method is suitable for classification of the images using spectral information. One can classify man-made objects such as roads and buildings using spectral signature. This information is useful for the preliminary change detection (Opitz, 2002a). Principle Component Analysis (PCA) method is a useful method for the detection of the changed pixels using remotely sensed digital images (Singh, 1989). This method use temporal images for the change detection and differentiate changed pixels from the unchanged pixels based on the radiometric differences. The PCA and supervised classification methods are useful for preliminary change detection (Phalke and Couloigner, 2004).

The preliminary change detection approach is a semiautomatic method. It is based on the classification of pixels of multispectral images using detailed and *a priori* knowledge about the area of interest (Oruc *et al.*, 2004). Classifying multispectral images

for preliminary change detection consists of drawing boundaries around geographically located classes that are homogeneous or acceptably heterogeneous, and of describing those classes with their attributes and their relations in a consistent and logical manner (Warren *et al.*, 1988). A multispectral sensor acquires multiple images of the same target object at different wavelength bands. Each band measures unique spectral characteristics about the target. By quantifying the spectral response of a known feature, it is possible to find out all occurrences of that feature within the image. Multispectral reflectance data, or remotely sensed imagery, from satellite sensors proved very useful for land-cover use, vegetation mapping, detailed soil mapping (in digital format) (Echavarria, 1996). Temporal information of these classified digital maps is very useful for preliminary change detection (Phalke and Couloigner, 2004).

Synthetic Aperture Radar (SAR) differential interferometry is very useful for detecting vertical and elevation changes in the target (Massonnet *et al.*, 1993). SAR technique uses phase information of the signals reflected back from the target for elevation estimation. SAR has an all weather mapping capability. These sensors hold a strong potential for change detection studies and can guaranty operational system even in presence of critical atmospheric circumstances and night (Mercier and Derrode, 2004). SAR image can be used for image classification and segmentation. SAR data has some limitations for change detections: for example, its poor spatial resolution leads to difficulty in change detection of man-made objects. Also, intensity values of a signal reflected from the same target are different for different generation of radar sensors (Girard-Arduin *et al.*, 2004). Back-scattering of radar signal from the target depends on the polarization, the wavelength of the signal, dielectric property of the target and the

incident angle. SAR is more useful for the detection of changes that occur with natural disaster earthquake or volcano eruption (Massonnet *et al.*, 1993).

The change analysis approach deals with the detection, analysis and quantitative assessment of changes in man-made objects. This approach is complex due to the need for manual supervision of the site and ground truth information. The change analysis approach is often based on 3-D geometric site model development (Agouris *et al.*, 2000) and detailed change detection using this model. The site model needs the following information for its development:

1. ground truth data of the area of interest;
2. the nature and size of the changes occurring;
3. the position of the actual change that has occurred;
4. the number of edges and corner points of the objects of interest; and
5. the elevation of the objects of interest.

A change analysis procedure deals with high resolution images and elevation information obtained from LIDAR, IFSAR DEM to obtain some of the above mentioned information. Thus it is suitable for the site model validation. The change analysis approach consists of steps: model to image registration, model validation, structural change detection and model update (Huertas and Nevatia, 1998). Change is obtained by comparing a 3-D model of the site prepared from old images, with new images.

When adopting these three approaches: preliminary change detection, microwave remote sensing and change analysis, for change detection of man-made objects, one needs to consider potential issues such as image registration and selection of threshold values, radiometric correction or calibration and accuracy assessment for change

detection (Deer, 1995). Digital change detection needs an accurate spatial registration of the multi-temporal images. It is observed that even small misregistration causes apparent widespread change over the entire image (Radke *et al.*, 2005). The selection of an appropriate threshold value for discriminating unchanged pixels from the changed pixels is also a key factor in most of the change detection methods (Hu *et al.*, 2004). It is necessary to make radiometric correction, calibration, standardization and normalization of the images for a separation of the changes of interest from the changes due to other factors, such as differences in atmospheric conditions, illumination, viewing angle or soil moisture (Deer, 1995). The calibration of different data images or sensors can be done by considering the spectral responses of unchanged regions as reference, for example water bodies. The spectral response of the reference region is expected to be less sensitive to difference in atmospheric condition, illumination, viewing angle and seasonal changes. An accuracy assessment of the derived changes is a very difficult task because by the time changes are determined in the area of interest, it is possible that few more changes have occurred. This makes it difficult to get accurate ground truth data for accuracy assessment.

To summarize, preliminary change detection methods are not suitable for the change detection of man-made objects due to its inability to define and categorize the derived change corresponding to the objects. Up to now change detection of man-made objects is difficult using SAR data due to its poor spatial resolution. However that may change with the arrival of high spatial resolution SAR imagery from Radarsat-2 and Terra SAR-X. Change analysis approach needs manual supervision and needs very expensive ground truth information for its implementation. Hence there is a need to

develop new reliable automated techniques for the change detection of man-made objects using VHR images. The new technique(s) also demand that the results of change detection are compatible for GIS data set update. This updated GIS data is useful for the city planning, property evaluation and taxation, among other purposes.

1.2 Research Objectives

The primary objective of this research is to detect changes in man-made objects such as building using VHR images in order to update GIS. The primary objective can be subdivided into the following tasks:

- a. implementation of existing methods such as supervised classification and principle component analysis method;
- b. studying the limitations and advantages of these existing methods; and
- c. development of a new automated technique for the feature extraction and change detection of man-made objects such as buildings;

The secondary objective of the research is to compare the existing techniques with the newly developed technique for change detection of buildings and to discuss the improvement in the overall results using information obtained with different detection techniques.

1.3 Thesis Organization

The organization of this thesis is as follows:

Chapter 2 describes the background of remote sensing. Various techniques available for change detection are reviewed, and the limitations and advantages of those techniques for the change detection of man-made object are also presented.

Chapter 3 examines different image processing techniques useful for feature extraction. This is necessary for the development of an efficient method for extracting man-made objects such as buildings. Edge detection, edge segmentation, determination of interesting points, such as corner points of buildings in the image is very useful for the feature extraction process (Phalke and Couloigner, 2005). Some of the interesting point detectors are also described in this chapter.

Chapter 4 implements and analyses traditional change detection methods such as post classification and Principle Component (PC) analysis. The results obtained using these traditional methods are presented and analysed.

Chapter 5 describes the newly developed 'L' shape template matching method for the extraction and change detection of buildings. The results obtained using the developed method is presented in this chapter. The developed method also implemented on the blue band of the pan-sharpen image.

Chapter 6 presents a quantitative comparison of the implemented methods for the change detection. This chapter discusses some of the advantages and limitations of the implemented methods for their qualitative comparison. It demonstrates the improvement brought by the new developed method.

Finally chapter 7 briefly summarize the research work and concludes. The recommendations and need of future work for the improvement of efficiency and reliability of the developed method is suggested.

Chapter 2

Literature Review

This chapter provides an overview of the available methods for change detection of man-made objects. The combination of knowledge from various areas of study such as: photogrammetry, remote sensing, GIS, computer science, and artificial intelligence, is required to solve various issues raised by the process of change detection. This overview presents theoretical background and various challenges inspiring this research.

2.1 Background

Since we are dealing with image based change detection, it is necessary to understand the parameters of a digital image and those affecting the process of change detection.

Resolution is an important parameter of digital images to define their characteristics. The characteristics of a digital imaging system can be described by four types of resolutions namely spatial, spectral, radiometric and temporal. These resolutions control the ability to interpret the image data. The spatial resolution dictates the amount of discernible details in the image. It gives us an idea of the smallest possible feature that can be detected in the image. It is mainly controlled by the Instantaneous Field of View (IFOV) of the sensor and flying height of the sensor with respect to the target (Habib, 2003). The spectral resolution describes the ability of the sensor to define fine or wide wavelength intervals. The finer the spectral resolution, the narrower the wavelength range for a particular channel or band. Fine spectral resolution facilitates fine discrimination between different targets based on their spectral response in each of the

narrow bands. The radiometric resolution of an image describes its ability to discriminate very slight differences in the recorded energy (Sato *et al.*, 2005). It is defined by the number of bits used for coding the recorded luminance. The temporal resolution is a measure of how often a given sensor acquired an image at the same location (Gautama and Goeman, 2004). It depends on the repeatability of the satellite orbit. It is important for disaster or environmental management and change detection application.

2.2 Challenges

Digital change detection deals with the quantification of temporal phenomena from multi-date imagery acquired by remote sensors. Digital change detection includes well defined digital methods. Examples of these methods are post classification comparison, image ratioing, image differencing, principle component analysis, differential snake, band discriminating transformation, differential interferometry (Byrne *et al.*, 1981; San *et al.*, 2004). These digital methods are not only able to extract information from the optical part but also from the non-optical part of the electromagnetic spectrum, such as infra-red and microwave. The derived change information using these digital change detection methods is difficult to replicate as different interpreters produce different results.

The change detection of man-made objects is a difficult task as most of these objects have similar spectral and shape properties. The available digital change detection techniques are based on the radiometric information and detect changed portion based on radiometric differences among the temporal images of the same location. These methods do not give any explicit information about the derived change. The optimum change

detection method need to identify if the derived change corresponds to man-made objects. It is also necessary that an optimum method should be able to categorize the change corresponding to man-made objects according to their type. For example the method needs to discriminate the changes in the roads from the changes in buildings. Digital methods such as post classification and Band Discriminating Transformation (BDT) are some of the available techniques for this task. Details of these techniques are given in section 2.3.1.3 and 2.3.1.4 of this chapter. These techniques are based on the spectral response of man-made objects. These methods can not provide information about change corresponding to individual man-made object. Secondly shadow effects, relief displacements, occlusions lead to false change detection of man-made objects such as buildings. Most of the research till now has been carried out for the change detection in an ecosystem and not on the change detection of man-made objects but the review of the change detection in an ecosystem is certainly helpful as a guideline for this research.

The ability of a system to detect and monitor changes in an ecosystem depends both on its capability to extract the geospatial information during a static situation and on its capacity to sense variability in the area of interest at one scale, for example: seasonal changes (Hobbs, 1990).

The main challenges for monitoring an ecosystem from space are (Coppin *et al.* 2004):

1. detecting changes due to two separate phenomena and quantification of the change (for example, quantify forest cover degradation due to seasonal change when changes can be due to human encroachment);

2. monitoring rapid and abrupt changes in addition to the progressive and incremental changes (for example, assess the impact of flood, drought or fire, versus a progressive expansion of agriculture. For an urban area changes due to urban sprawling versus changes due to disaster effects);
3. integrating the geospatial information obtained by different resolutions satellite images;
4. selecting the optimal temporal sampling rate for change detection;
5. pre-processing the data to reduce noise; and
6. registering accurately the temporal images acquired for the change detection.

The process of change detection using two remotely sensed images of a same location scanned at different times is known as bi-temporal change detection. Pre-processing for bi-temporal change detection consists of a series of sequential operations such as atmospheric correction or normalization, image registration, geometric correction, mosaicking, and subsetting. Direct comparison of these bi-temporal images is only possible after the radiometric adjustment and geometric correction such as orthorectification have been applied. Presence of the atmospheric effects, relief displacements, and radiometric differences will lead to false change information. When an absolute comparison between different temporal data is to be carried out, pre-processing is essential for the noise elimination. This is achieved by removing data acquisition errors, image noise or atmospheric errors (for example, portion of image covered by clouds) from the scene. This is necessary for reducing error occurring in derived change due to acquisition and atmospheric errors.

Many researchers have quantified the effect of misregistration on change detection. For example, when using 15 m spatial resolution, misregistration of 0.2 of a pixel resulted in 10 percent errors in change detection accuracies (Dai and Koharam, 1998). The misregistration causes positional difference in the same extracted feature from the temporal images. Change is derived by comparison of these extracted features based on their positional information. Change detection capabilities are very much limited by the spatial resolution of the image (Dai and Koharam, 1998). Misregistration causes degradation in feature matching events. Mainly it creates confusion in deciding between the change and no change boundaries (Radke *et al.*, 2005).

Common radiometric response varies in temporal images even when acquired by the same sensor. Variances in solar illumination conditions, atmospheric scattering and absorption affect the detector performance. Hence, the image needs to be normalized or, in other words, radiometric properties of the images need to be adjusted to those of a reference image (Kerekes and Landgrebe, 1989). Only through reliable radiometric calibration, a researcher can be confident that the obtained temporal, spatial changes are real and not artefacts introduced by differences in the calibration of sensors, or in the atmosphere or illumination (Coppin *et al.* 2004).

2.3 Change Detection Methods

For a detailed understanding of the pros and cons of the existing techniques of change detection, the existing change detection techniques are categorized into three groups: Image to Image, Image to GIS layer and Image to Geometric Site Model change detection. The following sub-sections review each group of techniques in detail.

2.3.1 Image to Image Change Detection

Image to Image change detection techniques use temporal geo-referenced images as an input for the detection of the change. Some of the image to image change detection methods are: Image Differencing, Image Ratioing, Post classification, Background Discriminant Transformation (BDT), Principle Component Analysis (PCA), and Fuzzy logic technique.

2.3.1.1 Image Differencing

Image differencing is one of the simplest digital algorithms for change detection. Image differencing means taking an image at one time and subtracting it from another image from a later time (Deer, 1995). The resultant image represents changes between the two dates. For example, each 8-bit band has digital values ranging from 0 to 255; the total potential range of the difference image is -255 to +255. Usually, a constant is added to the resulting value so that all differences are positive. Pixels exhibiting a significant radiance change are expected to lie in the tails of the distributions of the difference image, whereas the unchanged pixels should be grouped about the mean (Trisirisatayawong and Samchimchom, 2002).

Potential errors can be introduced by radiometric differences and poor registration of temporal images (Radke *et al.*, 2005). This method does not discriminate between differences due to scene changes and viewing effects. The bias and variance of errors are unknown and might be substantial. In that case simple image differencing techniques do not give an accurate detection of changes. Some form of radiometric standardization is normally applied to reduce the effect of illumination angle and intensity (including path

effects) and viewing angle. Image Differencing has been used in coastal studies, in temperate forests desertification and in the analysis of irrigated crops (Ha *et al.*, 2002).

2.3.1.2 Image Ratioing

Image ratioing is based on the ratio of the first image with respect to second. Final values can range from 0 to 255. To achieve equal possibility of getting a ratio between 1/255 to 1, and 1 to 255, the input temporal images must be normalized. The ratio values from 1/255 to 1 have reassigned values from 1 to 128 whereas the values from 1 to 255 have reassigned values from 128 to 255. In the areas where there is no change it is expected to obtain a normalized value of 128, while areas with large deviation from this normalized value represents the changes. A threshold is often used to filter out source variations (Deer and Eklund, 2002).

The main limitation of this method is that its performance depends on the statistical distributions of the input images. It was relatively successful when used to determine urban change (Todd, 1979). It has been stated that ratioing is less sensitive to multiplicative noise in SAR imagery than differencing (Weydahl, 1991). This method requires the determination of a threshold that will indicate when a change is significant. This method does not discriminate between differences due to scene changes and viewing effects. As this method works on a pixel level, neighbourhood viewing effects will appear as potential changes (Deer and Eklund, 2002).

2.3.1.3 Post Classification Comparison

The Post Classification Comparison (PCC) method performs a multispectral classification on each source image, and then compares the resulting classified images for differences (Howarth and Wickware, 1981). Classifications require human expertise to generate a classified image. One advantage of the post-classification comparison is that this method minimizes the search space and the effects of seasonal and atmospheric differences between the scenes. Post-classification comparison has been used to detect non-urban from urban or forest from crop land conversion, and changes in general land use such as wetland or forests (Cho, 2000).

The process of classification itself can be either supervised or unsupervised. The comparison of the classified images can be carried out visually, or by computer. A computer is better in quantitative analysis, but human operators are much better in discriminating patterns and shapes. The main disadvantage of the PCC method is that errors depend upon the accuracy of the training data sets used. Furthermore classification errors introduce spurious change detection. The spectral response of roads, buildings and parking lots are similar as shown in Figure 3.1. So precise extraction and change detection of these objects using classification technique is difficult (Phalke and Couloigner, 2004).

2.3.1.4 Background Discriminant Transformation (BDT)

The Background Discriminant Transformation transforms a multispectral image, similarly to a in the principal component transformation. The linear transformation coefficients are computed to maximize the variance (information content) of the non-

background (man-made) objects relative to the background objects (Shettigara *et al.*, 1995). BDT has properties of countering global and background changes and enhancing changes in the objects of interest. The method requires the user to identify the background class that needs to be suppressed in order to enhance the non background or the useful information. Any non-background or man-made object is expected to be uncorrelated to the background. The BDT procedure enhances the non-background objects naturally as it tries to maximize the non-background variance with respect to the background. Change detection can be obtained by comparing enhanced man-made object (non-background) information of available data sets (Forssén, 1997).

This technique has the advantage of counteracting the effects of global and background changes which often dominate the images and render the detection of changes in the objects of interest difficult. It is simple and efficient and can be implemented in systems for real time viewing of change-enhanced images (Forssén, 1997). The semi-automatic process of the classification step requires improvement as for example, in the case study by (Shettigara *et al.*, 1995), small portion of the background was marked as ‘man-made new’ objects. Misregistration in the images affects the performance of the clustering process as well, which reduces the accuracy of the change detection. An accuracy assessment is difficult as the sun-sensor object geometry creates artefacts of changes due to changes in shadows and shades of objects.

2.3.1.5 Principal Component Analysis (PCA)

The Principal Component Analysis (PCA) technique uses the Principal Components Transformation (PCT) to detect changes. PCT is a linear transformation which defines a

new, orthogonal coordinate system such that the data can be represented without correlation (Wiemker *et al.*, 1997). The axes of the new coordinate system are defined by the eigen vectors of the covariance matrices. Each individual pixel is transformed by vector multiplication of its original vector (*i.e.* pixel intensity value) and the eigen vectors, resulting in coordinates of a new data set of pixel vectors. In summary PCT transforms original intensity values of temporal data into a new parameter space. The orthogonal Principle Component one (PC1) and two (PC2), represent the axes of the new space. The PC1 axis represents the unchanged component while the PC2 axis represents the changes (Singh, 1989). Thus, PCA method is based on the idea that multi-temporal data are highly correlated, especially unchanged regions. So the change can be highlighted by rotating the data axes into the principal components maximizing the data variance. The PCA method gives information of the overall changed portions of the temporal images but does not give information about the type of change that has occurred in the object of the interest. Selection of appropriate threshold for change detection is crucial and largely influences the detection process. The details of this method are described in Chapter 4.

2.3.1.6 Fuzzy Logic

Fuzzy logic provides a mathematical formalism for combining evidence from various sources to estimate the significance of the detected changes (Deer and Eklund, 2002). Fuzzy logic can be applied on a pixel basis to generate a compound image which shows the type and degree of change for each pixel. It can also be used to combine groups of pixels into a single change, or to combine measurements such as size shape and colour of

a changed region into a single decision about whether or not the change has occurred.

Some recent work on fuzzy classification algorithms (Wang, 1990) using a fuzzy set membership approach offers promise of improvement in the accuracy of post classification comparisons. The fuzzy logic technique can be utilised to implement decision making process for detecting changed pixels. User need to set up rules for the discrimination of the unchanged pixels from the changed pixels. These rules are based on the information such as mean and standard deviation of the spectral values corresponding to the object of interest in the training data set. However, this process of change detection is not generalized and need to be trained each time for different data set (Deer and Eklund, 2002).

2.3.2 Image to Site Model Change Detection

Image to Site Model Type methods compare the object of interest extracted from the image with its geometric model. For the change detection of buildings, geometric models of building are developed using geo-physical information such as number of corner points, number of edges connecting those corner points, position, height, size and shape of the building. Housediff approach is one example of this type of techniques.

2.3.2.1 Housediff Approach

The Housediff approach combines edge detection and site model comparison (Huertas and Nevatia, 1998). Man-made object's change detection typically requires attention to changes in straight-line segments (walls, roads, and so on) including their emergence, disappearance, size and orientation changes, and the aggregation of those segments into

higher-level distinctive shapes (Agouris *et al.*, 2000). The Housediff technique is especially designed for detecting changes in 3-D building structures. This technique is based on few assumptions such as buildings are rectilinear and their composite shapes (such as 'L' or 'T') are described by their rectangular components. These assumptions allow us to have a uniform representation for the rectilinear shapes. Each exterior rectangular part of a building is represented by its 3-D wire-frame (consisting of 8 vertices and 12 edges). This 3-D wire-frame is referred to as site model. The camera geometry and the approximate viewpoint from which images are taken are assumed to be known. The Housediff approach for a change detection process consists of the following major steps (Huertas and Nevatia, 1998).

1. Site Model to image registration: Image to 3-D model registration using line feature matching technique.
2. Site Model Validation: Verifies whether the objects in the site model are present in the new image by comparing predicted features with observed features.
3. Structural Change Detection: Performs a detailed analysis of the possible changes using information of imaging and viewing conditions.
4. Site Model Updating: Updates the existing 3-D model if necessary.

The Housediff change detection engine tolerates imagery and vector data errors like misregistration, identifies small changes in both dimensions and automatically updates building vector data. However, the Housediff approach has few drawbacks:

1. It needs a visual inspection of the imagery data set
2. It requires information of the camera geometry and the location of the viewpoint, which are not easily available.

3. It is time consuming as it is a semi-automatic technique.

2.3.3 Image to GIS Change Detection

The image to GIS change detection method compares the extracted features with the feature of interest from GIS layers. For a direct comparison the features from GIS layer need to be converted into raster format. Then the derived changed information is obtained using feature matching technique. Differential snake is one of example of the image to GIS change detection. Image classification technique can also be useful for the Image to GIS change detection (Phalke and Couloigner, 2004).

2.3.3.1 Differential Snake

The differential snake technique is a novel technique that combines object extraction and change detection simultaneously. The differential snake technique is an extension of the deformable contour models (snakes) to be applied in a differential mode (Agouris *et. al*, 2000). The differential mode considers difference in the extracted features using snake technique as change. In this method any curvilinear objects such as roads can be extracted from the GIS data.

The energy function of a snake consists of internal and external forces. The internal forces regulate the ability of the contour to stretch or bend at a specific point while preserving some degree of geometric smoothness. The external force attracts the contour to specific image features. The snake model uses an energy minimization procedure to extract contour of the object of interest. The energy function contains all the basic performance information for the object extraction process (Agouris *et al.*, 2002).

The examination of function local values and gradients provides an estimate of the accuracy of the extraction. This accuracy information has been used as input for the differential snake model. Change detection can be achieved in the object extraction process itself by incorporating prior information (for example the last version of the shape of the road centerline and its corresponding accuracy estimates). The differential snake technique can perform a comparison of the image content to prior information to identify local or global changes, and to update the GIS information by means of versioning (Zhang and Couloigner, 2004). Versioning is defined as the process of improving the accuracy of the object information already stored in GIS even when no change has actually been detected.

This approach has few drawbacks such as the need of the initial position of the snakes, which makes it difficult to automate the process without the aid of existing GIS data. Another drawback is that a convergence problem may occur and requires much more time where, error in the detection of the feature's junction is known as convergence problem. The accuracy of the object extracted using the snake model depends on the selection of the start point of the model from which snake tracks object boundaries (Agouris *et al.*, 2001). This may lead to inaccuracies in the position of the extracted features and causing errors in the derived change detection.

2.4 Conclusion

It is observed from the literature review that there is no versatile method available which can deal with all three types of the tasks: change detection between Image to Image,

Image to GIS and Image to Site Model. Thus there is need for the development of new technique which will be suitable for the all three types of change detection.

The existing Image to Image change detection techniques are based on the spectral properties of the objects. Various parameters such as the selection of appropriate threshold, the radiometric adjustment of the images, the misregistration of the images, the selection of the training data set, and heterogeneity of the test site affect the performance of the change detection techniques. The existing techniques are semi-automated or manual techniques and need expert operators for the selection and adjustment of different parameters depending upon the technique used. Also, results obtained using the existing techniques are not often compatible with GIS data and hence are not always suitable for the GIS update.

Existing Image to GIS change detection method such as differential method is a useful change detection of the curvilinear features such as roads. However this method does not assign an identification value to each extracted feature. GIS update needs information in the digitized format and each feature should have a separate identification value. Secondly this method is not suitable for the extraction of linear features such as buildings with sharp corners.

Existing Image to Site Model based change detection method such as the Housediff approach is semi-automated and needs expensive ground truth information from the user for its implementation. Thus it is necessary to develop a new reliable, automated feature extraction based approach for the change detection of man-made objects which does not use expensive resources.

The preliminary objective of the research is to detect the change in man-made objects such as buildings and its application for GIS update. There is no suitable method for this task and thus a new method needs to be developed. The new method should be versatile and useful for all three types of change detection such as Image to Image, Image to GIS and Image to Site Model.

Chapter 3

Feature Extraction

3.1 Introduction

To identify a feature of interest, it is necessary to classify all the individual pixels, which correspond to that feature in one unique class. This process of classification is known as feature extraction. Feature extraction uses spectral, geometric or textural property of the feature for its extraction. Special colour or tone, gradient defines its spectral property. Edge, size, shape of the feature defines its geometric property. Pattern, spatial frequency, and homogeneity define its textural property (JARS, 1996).

The process of feature extraction can be divided into three stages: low, medium and high level feature extraction stages. Image classification is a traditional low level stage for the feature extraction since it classifies a set of similar objects as a single feature and does not further classify them as individual objects. The medium level stage of feature extraction deals with boundary detection and corner point detection, the outcome of which is then used to reconstruct the individual objects of the features obtained from the low level stage (Phalke and Couloigner, 2005).

The medium and high level stages are highly dependent on the set of features provided via the low level feature extraction stage (Opitz, 2002b). Detailed object extraction is carried out in these medium and high level stages. Detailed object extraction process assigns separate identification value to each extracted object. It also defines the object in a binary format, *i.e.* a predefined pixel value is assigned to boundary pixels of

the object and a zero pixel value is assigned to non boundary pixels. These stages suffer if there are too many or too few features (Schyns *et al.*, 1998). Too few features lead to insufficient data for the validation and too many cause uncertainty. In case of too many objects the process of feature extraction considers a group of closely located objects as one object. Feature extraction techniques based on edge detection are facing these difficulties. The high level extraction stage symbolizes the individual objects for identification purposes. The extracted features at high level stage can be grouped together to form a complete feature layer (Ohlhof *et al.*, 2000). A final step will verify the developed layer via comparison and confirmation against a pre-registered layer of GIS data.

3.2 Low Level Feature Extraction

The information obtained about the feature at the low level stage can not completely define a feature but it is very useful as a guiding tool for a more detailed feature extraction. This stage simply categorizes different types of features into classes. Every feature has attributes such as shape, size, colour, or texture pattern. The low level stage only uses properties of the spectral response of the features for the extraction process. It is impossible to extract many man-made features just based only on their spectral information. Different types of features, such as: roads, parking lots and buildings, constructed with similar material gives similar spectral response and hence get classified into a same class. For example, the highlighted portion of the classified image in Figure 3.1 represents roads misclassified as buildings. Using only the spectral information is not appropriate for an accurate feature extraction. Feature analysis has been newly developed

as a low level feature extraction technique. This technique is used as preliminary feature extraction process. This algorithm automatically develops information that correlate the known data with the target features (Opitz, 2002a). The extraction of man-made objects such as buildings needs VHR images for accurate extraction. The panchromatic images of the satellites Quickbird and IKONOS are suitable for this purpose due to very high spatial resolution: 0.7 m and 1 m respectively. Multispectral images are useful for the image classification as they cover more spectral information. However they have a lower spatial resolution than the panchromatic images: 2.8 and 4 m, respectively. It is difficult to precisely define shape and edges of small objects such as buildings from the classified images obtained using multispectral images due to their poor spatial resolution. Thus data fusion of the panchromatic and multispectral images is useful as it provides us output image with multiple spectral bands and of spatial resolution identical to the panchromatic image.

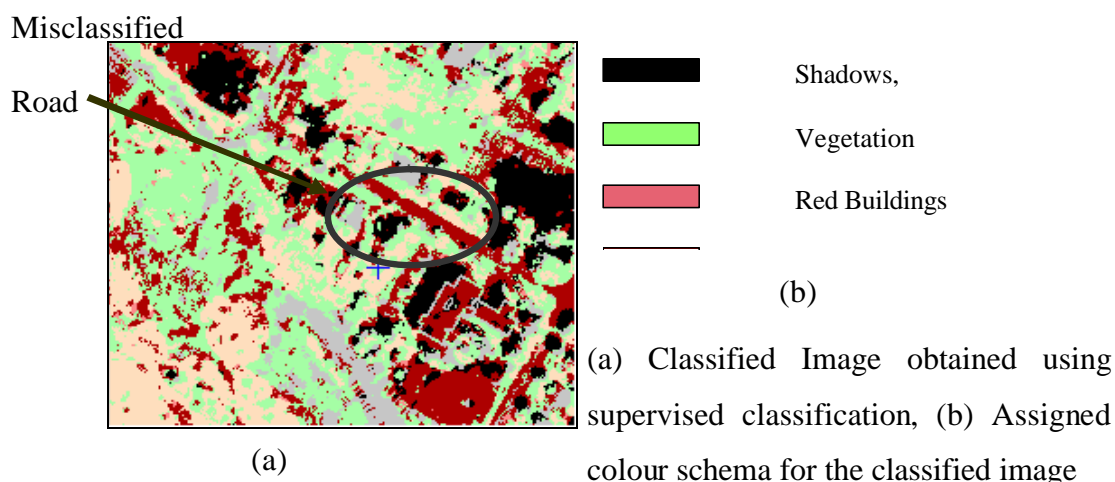


Figure 3.1 Example of misclassification

Image fusion is the process of integration of different images of same location acquired by different sensors. One of the objectives of image fusion is to obtain a higher spatial and spectral resolution image using the high spatial resolution image as reference. The higher spatial resolution improves visual interpretation ability. Image fusion can be at different levels namely pixel level, feature level or object level. For classification purpose pixel level data fusion is preferred. Some popular methods for image fusion are Principle Component (PC) analysis, High-Pass-Filter (HPF), Intensity Hue Saturation transform (IHS) and wavelet transformation method. PC analysis and IHS consider all bands of the multispectral images for the fusion whereas HPF and wavelet transformation considers information of individual channels for the fusion (Hoàng *et al.*, 2004; Meenakshisundaram and Couloigner, 2004).

3.2.1 Principle Component Analysis Method for Image Fusion

Principle Component (PC) analysis uses linear transformation of multispectral data. In this linear transformation, intensity values are re-projected on new orthogonal axes: principle component one and principle component two. The PC one of the multispectral image is replaced by the PC one of the higher spatial resolution image. Then to retain the spectral information of the multispectral data the inverse transformation is carried out which transforms the PCs back to the original multispectral data but with a higher spatial resolution (Lillesand and Kiefer, 2000; Wald, 2002).

3.2.2 Intensity Hue Saturation (IHS)

This is a simple technique for image fusion. IHS transforms Red, Green, and Blue (RGB) bands of a multispectral image into Intensity, Hue and Saturation. These transformed IHS values represent three different orthogonal attributes (Harris and Stephens, 1988). For the fusion of multispectral image bands with panchromatic image first one needs to select any three bands from multispectral image. Secondly, Intensity of multispectral bands is replaced by the panchromatic image. This gives new IHS characterized multispectral image. The inverse transformation of this IHS transformed image back to RGB gives a new multispectral image which retains the spectral information of the original image while its spatial resolution became identical as the panchromatic image one.

3.2.3 High Pass Filter

The High Pass Filter (HPF) consists of three basic steps: Performing high pass filter on the high spatial resolution image, Performing low pass filter on the multispectral image for extraction of spectral information, and Deriving weighted sum of the high and low pass filter results to obtain fused image with same spectral information and high spatial resolution. (Chavez *et al.*, 1991) observed that HPF method exhibits less distortion in the spectral characteristic of the data compared to IHS and PCA techniques.

3.3 Medium and High Level Feature Extraction

The process of region boundary detection is considered as a medium level feature extraction and the boundary detection of individual small (man-made) objects as a high level feature extraction. Various methods such as differential snake or BDT exist for

medium and high level feature extractions (Forssén, 1997). Edge-based segmentation is a popular medium level feature extraction method (Dow *et al.*, 2004). A combination of edge-based segmentation and corner detector methods are useful for the high level feature extraction (Phalke and Couloigner, 2005).

3.3.1 Edge-based Segmentation

Edge-based segmentation techniques rely on the edges provided by edge detector operators. Discontinuities in the detected edges, edge blurring or double edging affect the result of an edge-based segmentation. The presence of edges at locations where there is no border and undetected edges where there is a border, are two of the most common problems in edge-based segmentation. This segmentation not only will detect edges but will also combine edge segments to form edge chains that will contribute to better boundaries of the features present in the image.

3.3.2 Edge Detection

Edge detection defines the boundaries of man-made objects. It is the essential first step of the feature extraction process. The process of feature extraction using digital imaging needs detailed understanding of the edge detector operators. An edge can be represented as a set of connected pixels that lie on the boundary between two distinct regions. In digital images object boundaries show rapid changes in the gray levels within a small area of an image as shown in Figure 3.2, yielding discontinuity of gray level function. This discontinuity function is considered as an edge. Thus the detection of edge pixels is derived from determining the local discontinuities of the gray level. Since difference

between the gray level values of neighbouring pixels defines this discontinuity the operator needs to decide an appropriate threshold for the difference value to detect the edge pixels. Edge detection requires the ability to measure gray-level transitions. However, most of the times the transition of the gray level along the edge is not sharp but smooth. Figure 3.2a shows that the cross-section of edge has the shape of a ramp. This is due to the imperfection of image acquisition which blurs out the edges or due to a spatial resolution coarser than the scale at the location of the edge. The thickness of the edge detected by an edge detector depends on this width of transition (ramp). Figure 3.2b is an example showing thick extracted edges due to ramp transition of the gray level at the edges. There are many existing edge detectors such as Sobel (Sobel, 1990), Canny (Canny, 1983; 1986), Laplacian (Mortenson and Barrett, 1998) or Prewitt (Prewitt, 1970). These edge detectors can be broadly categorized into first and second order derivative edge operators. Sobel and Prewitt are examples of first order derivative edge detectors whereas Laplacian is example of second order edge detector.

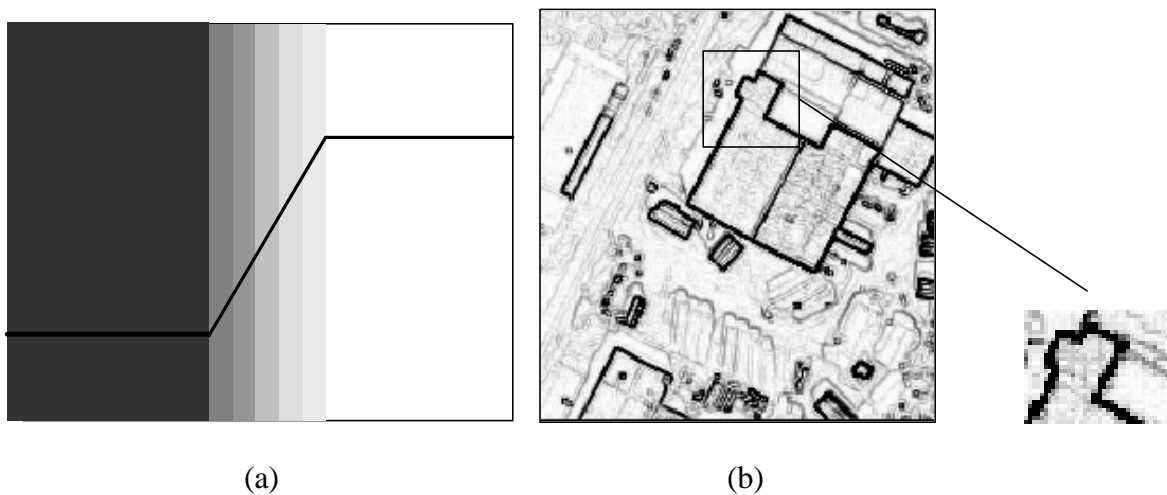


**Figure 3.2 (a) Gray level variations along the edge and its effect on detected edges
(b) Example showing effect of gray level variation on detected edges**

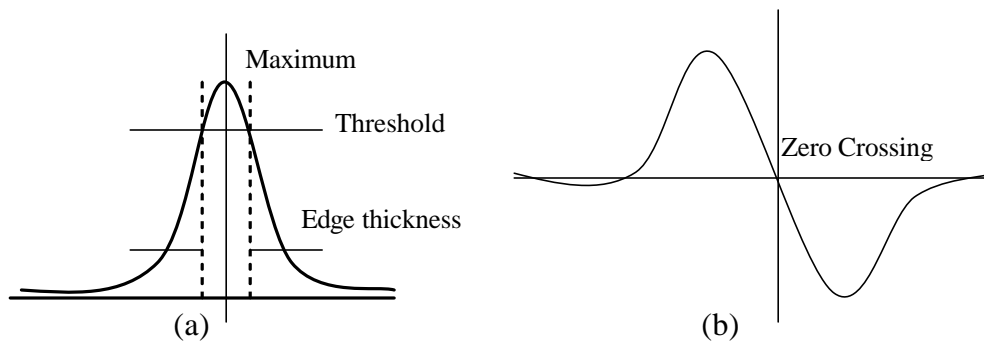


Figure 3.3 First and second derivatives of a function (a) Represents first derivative of the edge (b) the second derivative of the edge

3.3.3 Edge Detection Using First Order Derivatives

The derivative of a digital pixel grid can be defined in terms of differences. The first derivative of an image containing gray value pixels must fulfill the following conditions: it must be zero in flat segments, *i.e.* in area of constant gray-level values; it must be nonzero at the beginning of a gray level step or ramp; and it must be non zero along the ramp (constant change in gray values).

The first-order derivative of one-dimensional function $f(x)$ can be obtained using equation 3.1.

$$df / dx = f(x + 1) - f(x) \quad (3.1)$$

An image is a function of two variables $f(x, y)$. Equation 3.1 only refers to the partial derivative along the x axis. Pixel discontinuity can be determined along eight possible directions such as: up, down, left, right and along the four diagonals. The variation in the value of df / dx (gray value) along the edge is represented by the waveform shown in

Figure 3.3a. The x axis represents the pixel spacing along the 'x' axes and 'y' axis represents the gray level gradient.

The response of the first order derivative operator along the edge is as shown in Figure 3.3a. The peak of the response corresponds to the edge pixels. Determination of exact pixels corresponds to the peak is difficult task. It is general practice to use appropriate threshold (based on trial and error, refer Figure 3.3a) and all the pixels having response greater than the threshold are considered as edge pixels. The response shows smooth transition at the peak. This causes the neighbouring pixels of the edge to be also considered as edge pixels. Edges derived using first order derivative operators are thick.

3.3.4 Edge Detection Using Second Order Derivative

Second order derivative needs to fulfill the first two points of first derivative and it should satisfy following conditions:

1. it must be zero along the ramp ;
2. it produces two values for every feature;
3. straight line joining the extreme positive and negative values of second derivative across the edge would cross at of the edge; and
4. sign of the second derivative can be used to determine whether an edge pixel lies on the dark or the light side of the edge.

Second order derivative is represented by the equation:

$$d^2 f / d^2 x = f(x + 1) - f(x - 1) - 2f(x) \quad (3.2)$$

As shown in equation 3.2, second order derivative considers two neighbouring pixels, one from each side of the gradient detection. This leads to two sharp transitions in the $d^2 f$ value at the edges in the image.

The graphical representation of this transition appeared as a sinusoidal wave (Figure 3.3b). The position of the zero crossing (of this sinusoidal wave) gives us the position of the edge in the input image. The nature of the second order derivative response at the edge is sharp. This eliminates the possibility of detecting neighbouring pixels as edge pixels. Second order derivative produces thin edges.

3.3.5 Comparison of First and Second Order Derivative Operators

As per experiments conducted by (Gonzalez and Woods, 2001) using first and second order derivative methods, the results conclude that:

“First order derivatives generally produce thicker edges in an image. Whereas, second order derivatives have a stronger response to fine detail, such as thin lines and isolated points. First order derivatives generally have a stronger response at step changes in gray level step. Second order derivatives produce a double response at step changes in gray level”.

3.4 Corner and Interesting Point Feature Detection

Most of the work on two-dimensional features extraction is focused on corner detection, where boundary curvature is significantly high (Quddus *et al.*, 1999). These corner points in addition to the edges corresponding to the boundary of objects are useful for reconstructing each object.

According to Forstner, (1987), the properties of corner (interesting) points which are suitable for feature extraction are:

1. Invariance: The corner points are found to be invariant with geometric and radiometric distortions.
2. Distinctness: They are distinct. Distinctness is measured by comparing the correlation coefficient of the point with its neighbouring pixels. If the maximum of correlation coefficient is small, then the point is considered as dissimilar thus a distinct point.
3. Stability: The position of the corner points is found to be well defined and stable. The stability of the corner point is only affected by the occlusion and by an improper orthorectification.
4. Uniqueness: The distinct point property is local and uniqueness is global. This is to avoid the locally distinct but repetitive features. This is necessary to avoid confusion and inaccuracy in the matching process. Most of the time it is difficult to find unique points in the image. Corner points do not independently possess this property but the combination of corner points and edge segments is found to be unique (Forstner, 1994).

The interesting points, *i.e.* the corner points, are also useful for the determination of geometric transformation between two similar images. Detecting the corresponding point in two similar images is a challenging task; this can be simplified using epipolar line information (Schenk, 1999). For orthorectified or registered images, the position of the corresponding interesting point in the images is the same. Thus detection of the

corresponding interesting point in the orthorectified or registered images is a simpler process.

There are various existing corner detection operators. The Moravec interest operator (Moravec, 1979), the Plessey operator (Harris and Stephens, 1988), or the Forstner operator (Forstner, 1994) are some examples. These operators are mainly divided into two categories: template-based and geometry-based corner detectors. Template-based corner detectors use a template matching technique for the corner detection. Geometry-based corner detectors measure the differential geometry features of corners (Montesinos *et al.*, 1998).

The input to the corner detector operator is a gray-level image; the output grid contains values representing the probability of each pixel to be a corner point (Smith, 1992). The interest points are in fact image locations where the interest operator computes a high variance value (Habib, 2003). From Figure 3.4, it is observe that a significant change in gray level values occurs at the interesting points. Hence most of the interesting point operators are based on the detection of high variance point within an image.

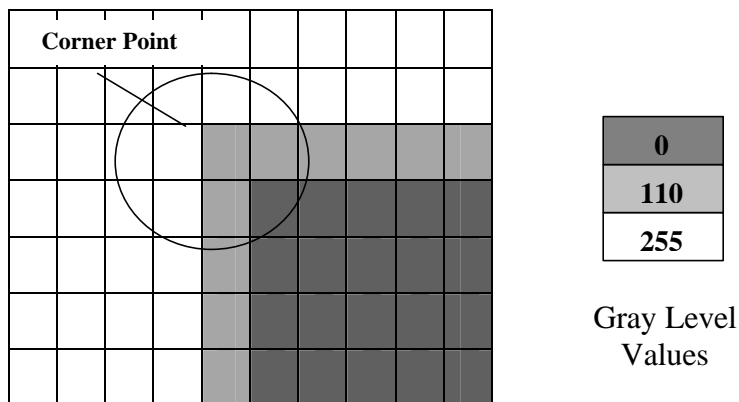


Figure 3.4 Gray level variations around the interesting point

A corner detector should satisfy the following criteria: “A corner detector should detect all the actual corner points present the image. It should be reliable and no faulty corner points should be detected. Also, detected corner point position must be well defined and as accurate as possible. Finally corner detector should compensate for noise and it should be fast and efficient” (Moravec, 1979).

The following is a brief description of few existing corner detectors:

3.4.1 Moravec Interest Operator

As the first step, the Moravec operator (Moravec, 1979) determines the variances along the left, right, up and down directions. I_1, I_2, I_3, I_4 represent the variance along these four directions within the window of interest, given by:

$$I_1 = \sum_{(x,y) \in S} [f(x,y) - f(x, y+1)]^2$$

$$I_2 = \sum_{(x,y) \in S} [f(x,y) - f(x+1, y)]^2$$

$$I_3 = \sum_{(x,y) \in S} [f(x,y) - f(x+1, y+1)]^2$$

$$I_4 = \sum_{(x,y) \in S} [f(x,y) - f(x, y-1)]^2$$

$$I(x_c, y_c) = \min(I_1, I_2, I_3, I_4) \quad (3.3)$$

where S represents all the pixels in the 3 X 3 window surrounding the central pixel (x_c, y_c) and $f(x, y)$ represents the intensity value of pixel at (x, y) position. From equation 3.3, one can see that the minimum value of the directional variances is considered as the interest value at the central pixel, (x_c, y_c) . This central pixel is a corner point if and only if it is a

local maximum (Habib, 2003). It is necessary to remove all the isolated points in the image before applying the Moravec operator. These isolated points or noisy pixels could have a high variance and the Moravec operator may then consider them as interesting points (Moravec, 1979).

3.4.2 Harris/Plessey Corner Detector

The Harris detector (Harris and Stephens, 1988) computes the locally averaged moment matrix ' M ' from the image gradient given by:

$$M = \begin{bmatrix} \left(\frac{\partial I}{\partial x}\right)^2 & \left(\frac{\partial I}{\partial x}\right) \left(\frac{\partial I}{\partial y}\right) \\ \left(\frac{\partial I}{\partial x}\right) \left(\frac{\partial I}{\partial y}\right) & \left(\frac{\partial I}{\partial y}\right)^2 \end{bmatrix} \quad (3.1)$$

where $I(x, y)$ is the intensity value of the pixel (x, y) . The elements of ' M ' represent local gradients. Eigen values of the matrix ' M ' are used for determining the corner points. These eigen values represent the local variances of the image. Smaller eigen values represents constant intensity or a low variation portion of the image. If one of the eigen values is small and another is large, the local variance is in one direction. This is the property of an edge where the variance is high in the orthogonal direction of the edge. On the other hand it is low along the direction of the edge. If both eigen values are high, the local variance in any direction changes sharply and that indicates a corner point. The corner response function is given by equation 3.4:

$$R = \det M - k(\text{trace}(M))^2 \quad (3.4)$$

where, constant parameter k is a set to 0.04, which controls the magnitude of corner response (Harris and Stephens, 1988). The corner is defined as the local maximum of the corner response function.

3.4.3 Smallest Univalued Segment Assimilating Nucleus (SUSAN) Corner Detector

The SUSAN operator (Smith and Brady, 1997) uses a circular mask or kernel for the corner detection. The brightness of each pixel within a kernel is compared with the brightness of that kernel's center. An area of the kernel which has the same (or similar) brightness as the center can be defined as a Univalued Segment Assimilating Nucleus (USAN). It contains information about the shape and size of the feature. Boundaries of the feature can be detected using the size, centroid and edges of the USAN.

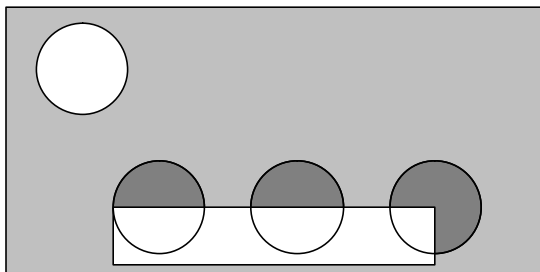


Figure 3.5 Corner detection using circular SUSAN kernel (Smith and Brady, 1997)

As shown in Figure 3.5, the area of USAN reaches half of the area of kernel when the nucleus of the kernel lies on the boundary of the feature. This area falls to less than half when nucleus lies on a corner of the feature. This property of an USAN's area is used to determine the presence of edges and corner points (Smith and Brady, 1997).

Therefore to find the corner point, a threshold is set to exactly half of the maximum area. Sometimes due to the blur boundaries between regions the Susan operator provides false corner point (Smith, 1992; Smith and Brady, 1997).

The Susan operator is also used as edge detector. The places where the sharp change in brightness occurs are considered as edges. This method for corner and edge detection is neither based on the first nor second order image derivative.

3.4.4 Forstner Corner Detector

The Forstner operator (Forstner, 1994) fulfills all the requirements of the interesting points which are distinctness, invariance, stability, uniqueness and interoperability. The extraction of the interesting points can be carried out in three steps:

1. selection of the optimal window;
2. classification of the image function within the selected window; and
3. estimation of the optimal points within the optimal window.

The selection of the optimal size window for the corner detection is based on the average gradient magnitude within the window of a pre-specified size. The classification differentiates corner points from other singular points such as isotropic texture or rings. Finally it precisely estimates the optimal corner point position.

Let the $m_r \times m_c$ window contain the corner point $p_o = (r_o, c_o)'$. The Forstner operator estimates the corner point $\hat{p}_o = (\hat{r}_o, \hat{c}_o)$.

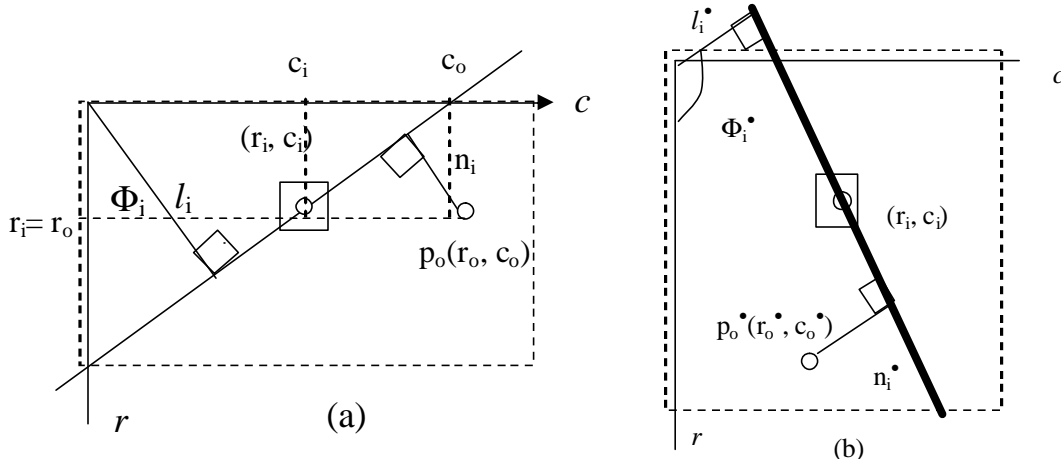


Figure 3.6 Model for estimating corners and center of the circular symmetric feature (Forstner, 1994) (a) The edge element through (r_i, c_i) is represented by a straight line (l_i, F_i) . (b) The slope element through (r_i, c_i) is represented by the straight line (l_i^*, F_i^*) .

From Figure 3.6a we obtained equation 3.5:

$$l_i = \cos \mathbf{f}_i \cdot \hat{r}_0 + \sin \mathbf{f}_i \cdot \hat{c}_0 + n_i \quad i=1, \dots, m \quad (3.5)$$

This equation is assumed to hold for all $m = m_r \times m_c$ pixels (r_i, c_i) . The weight of l_i is assumed to be w_i given by equation 3.6:

$$w_i = \|\nabla f_i\|^2 = f_r^2(r_i, c_i) + f_c^2(r_i, c_i) \quad (3.6)$$

where $f_r(r_i, c_i) = \frac{\partial \hat{g}(r_i, c_i)}{\partial r}$, $f_c(r_i, c_i) = \frac{\partial \hat{g}(r_i, c_i)}{\partial c}$ and \hat{g} is the intensity values in the

image.

Minimizing $\Omega(r_0, c_0) = \sum_{i=1}^m n_i^2 \cdot w_i$ with respect to \hat{r}_0 and \hat{c}_0 gives the following equations:

$$\frac{1}{2} \frac{\partial \Omega(\hat{r}_0, \hat{c}_0)}{\partial \hat{r}_0} = \sum_{i=1}^m \cos \mathbf{f}_i \cdot (l_i - \cos \mathbf{f}_i \cdot \hat{r}_0 - \sin \mathbf{f}_i \cdot \hat{c}_0) \cdot w_i = 0 \quad (3.7)$$

$$\frac{1}{2} \frac{\partial \Omega(\hat{r}_0, \hat{c}_0)}{\partial \hat{c}_0} = \sum_{i=1}^m \sin \mathbf{f}_i \cdot (l_i - \cos \mathbf{f}_i \cdot \hat{r}_0 - \sin \mathbf{f}_i \cdot \hat{c}_0) \cdot w_i = 0 \quad (3.8)$$

This leads to the normal equation in matrix format:

$$\begin{bmatrix} \sum_{i=1}^m w_i \cos^2 \mathbf{f}_i & \sum_{i=1}^m w_i \cos \mathbf{f}_i \sin \mathbf{f}_i \\ \sum_{i=1}^m w_i \cos \mathbf{f}_i \sin \mathbf{f}_i & \sum_{i=1}^m w_i \sin^2 \mathbf{f}_i \end{bmatrix} \begin{bmatrix} \hat{r}_0 \\ \hat{c}_0 \end{bmatrix} = \begin{bmatrix} \sum_{i=1}^m l_i w_i \cos \mathbf{f}_i \\ \sum_{i=1}^m l_i w_i \sin \mathbf{f}_i \end{bmatrix} \quad (3.9)$$

Replacing l_i by $r_i \cos \mathbf{f}_i + c_i \sin \mathbf{f}_i$, and f_{r_i} by $f_r(r_i + c_i) = \|\nabla f_i\| \cos \mathbf{f}_i$

and f_{c_i} by $f_c(r_i + c_i) = \|\nabla f_i\| \sin \mathbf{f}_i$, equation 3.9 becomes:

$$\begin{bmatrix} \sum_{i=1}^m f_{r_i}^2 r_i & \sum_{i=1}^m f_{r_i} f_{c_i} \\ \sum_{i=1}^m f_{r_i} f_{c_i} & \sum_{i=1}^m f_{c_i}^2 c_i \end{bmatrix} \begin{bmatrix} \hat{r}_0 \\ \hat{c}_0 \end{bmatrix} = \begin{bmatrix} \sum_{i=1}^m f_{r_i}^2 r_i + f_{r_i} f_{c_i} c_i \\ \sum_{i=1}^m f_{c_i}^2 c_i + f_{r_i} f_{c_i} r_i \end{bmatrix} \quad (3.10)$$

We can also rewrite equation 3.10 as follows:

$$\left(\sum_{i=1}^m W_i \right) \hat{p}_0 = \sum_{i=1}^m (w_i p_i) \quad (3.11)$$

where the singular-weights matrices are given by:

$$W_i = \nabla f_i \nabla f_i' = \|\nabla f_i\|^2 \cdot e_i e_i' = \|\nabla f_i\|^2 \cdot \begin{pmatrix} \cos^2 \mathbf{f}_i & \cos \mathbf{f}_i \sin \mathbf{f}_i \\ \cos \mathbf{f}_i \sin \mathbf{f}_i & \sin^2 \mathbf{f}_i \end{pmatrix} \quad (3.12)$$

Similarly from Figure 3.6(b), we obtain equation 3.14, 3.15 and 3.16 as:

$$l_i \cdot = \cos \mathbf{f}_i \cdot \hat{r}_0 \cdot + \sin \mathbf{f}_i \cdot \hat{c}_0 \cdot + n_i \cdot \quad i=1, \dots, m \quad (3.13)$$

$$\begin{bmatrix} \sum_{i=1}^m w_i \cos^2 \mathbf{f}_i & \sum_{i=1}^m w_i \cos \mathbf{f}_i \sin \mathbf{f}_i \\ \sum_{i=1}^m w_i \cos^2 \mathbf{f}_i & \sum_{i=1}^m w_i \cos^2 \mathbf{f}_i \end{bmatrix} \begin{bmatrix} \hat{r}_0^\bullet \\ \hat{c}_0^\bullet \end{bmatrix} = \begin{bmatrix} \sum_{i=1}^m l_i^\bullet w_i \cos \mathbf{f}_i \\ \sum_{i=1}^m l_i^\bullet w_i \sin \mathbf{f}_i \end{bmatrix} \quad (3.14)$$

$$\begin{bmatrix} \sum_{i=1}^m f_{r_i}^2 r_i & -\sum_{i=1}^m f_{r_i} f_{c_i} \\ -\sum_{i=1}^m f_{r_i} f_{c_i} & \sum_{i=1}^m f_{r_i}^2 \end{bmatrix} \begin{bmatrix} \hat{r}_0^\bullet \\ \hat{c}_0^\bullet \end{bmatrix} = \begin{bmatrix} \sum_{i=1}^m f_{r_i}^2 r_i + f_{r_i} f_{c_i} c_i \\ \sum_{i=1}^m f_{c_i}^2 c_i + f_{r_i} f_{c_i} r_i \end{bmatrix} \quad (3.15)$$

$$\left(\sum_{i=1}^m W_i^\bullet \right) p_0^\bullet = \sum_{i=1}^m (w_i^\bullet p_i) \quad (3.16)$$

where the singular-weights matrices are given by:

$$W_i^\bullet = \|\nabla f_i\|^2 e_i^\bullet \cdot e_i^\bullet = \|\nabla f_i\|^2 \begin{pmatrix} \cos^2 \mathbf{f}_i & -\cos \mathbf{f}_i \sin \mathbf{f}_i \\ -\cos \mathbf{f}_i \sin \mathbf{f}_i & \sin^2 \mathbf{f}_i \end{pmatrix} \quad (3.17)$$

The test statistic for the corner point detection is given by equation:

$$T = \frac{\Omega}{\Omega^\bullet} \quad (3.18)$$

where,

$$\Omega = \sum_{i=1}^m (r_i - \hat{r}_0, c_i - \hat{c}_0) \cdot W_i \cdot (r_i - \hat{r}_0, c_i - \hat{c}_0)' = \sum n_i^2 w_i \quad (3.19)$$

$$\Omega^\bullet = \sum_{i=1}^m (r_i - \hat{r}_0^\bullet, c_i - \hat{c}_0^\bullet) \cdot W_i^\bullet \cdot (r_i - \hat{r}_0^\bullet, c_i - \hat{c}_0^\bullet)' = \sum n_i^{\bullet 2} w_i^\bullet \quad (3.20)$$

If the value of 'T' is significantly smaller than 1 then the point is considered as a corner point (Forstner, 1994).

3.5 Conclusion

Various methods for edge and interesting point (corner) detection have been studied. The type 1 Laplacian edge detector operator is a second order derivative edge detector. It provides very thin edges. On the other hand Sobel edge detector is a first order derivative type. It represents edges with thick lines. The purpose of preliminary edge detection is to get the information about the shape and location of the objects boundaries. Derived preliminary edges need to be sharp and noise free as they are used as a guiding tool for detail edge detection. The detail edge detection process needs to derive information about all missing edges of the preliminary detected boundaries of the objects. Thus detail edge detection process needs to provide information about all the edges present in the image. First order edge detectors are more suitable for this purpose as they have an ability to detect small transition in the intensities at the location of the edges. The Laplacian edge detector is useful for a preliminary edge detection of man-made object and the Sobel edge detector is useful for a more detailed feature extraction.

It is observed that the Forstner corner detector is a reliable method for the detection of corner points. This operator can be directly used on the VHR images without any pre-processing and provides sub pixel level positional accuracy.

Chapter 4

Traditional Change Detection Methods

4.1 Preliminary Change Detection

The process of change detection of man-made object is widely divided into two stages such as preliminary and detailed change detection. This chapter describes preliminary change detection methods. The selected existing methods for this purpose are implemented for image to GIS change detection and image to image change detection. The post classification and Principle Component Analysis (PCA) methods are presented, as methods for preliminary change detection. The post classification method is used for image to GIS change detection. The PCA method is implemented for image to image change detection. Image to site model type of change detection method is not implemented as it needs expensive and time consuming ground truth data (Huertas and Nevatia, 1998). The results obtained using the implemented methods are also presented and analysed in this chapter.

Post classification based change detection performs multispectral classification on each source image, and then compares the resulting images for differences in classification (Howarth and Wickware, 1981). The results obtained using this method show that it is better in handling effects of biases and variance between images. However, the main disadvantage of this method is that errors in classification have compounding effects. Common classification errors (Figure 3.1) introduce also spurious change detections (Pilon *et al.*, 1988). This method is selected as a preliminary change detection

method as it provides initial information about the location and size of man-made objects such as roads, buildings and parking lots. The information about each type of objects is then stored in separate layers. One can then compare the feature layer obtained using post-classification method and the corresponding GIS data set layer to detect the changes.

The PCA method has been selected for the preliminary change detection as it is useful in multi-temporal data set since standardization minimizes the differences due to atmospheric conditions or sun angles (Deer, 1995). It is computationally efficient, reliable and accurate method for change detection.

4.2 Data Set Used

The data sets used for this research are:

- The Ikonos Panchromatic (1 metre spatial resolution) and multispectral imagery (4 metre spatial resolution) of year 2001 and 2002 acquired over the City of Fredericton, New Brunswick, Canada.
- The layers of interest from the Canadian National Topographic Data Base (NTDB) for the City of Fredericton (Scale 1:50 000) of year 1995.

4.3 Pre-Processing Steps

The Ikonos image data set used is taken over the span of one year. The temporal difference leads to radiometric difference and misregistration. However, the Ikonos images used are orthorectified with the precision of 0.9-2.0 metres (Wang and Ellis, 2005). Nevertheless it is observed that there are small misregistrations of 0.4 pixels in the

Ikonos panchromatic temporal images used for the research. The traditional change detection methods such as post-classification and PCA methods determine changes at the pixel-level. Thus, normalization of the images is necessary to bring the intensity values of the temporal images to the same level. It is also necessary to perform histogram equalization for better interpretation of the image. It can be crucial for the selection of accurate training data for the classification of images. The histogram equalization also helps in interpreting the derived change information as it enhances the visualization ability of the operator. The change detection technique such as PCA only gives information about changed pixels in the temporal images and user needs to interpret the change that corresponds to the object of interest.

A small subset of the Ikonos panchromatic images of the city of Fredericton, New Brunswick, Canada year 2001 is presented in Figure 4.1a. This image is of poor contrast and it is very difficult to interpret its information content. The enhanced image is obtained using the histogram equalization.



Figure 4.1(a) Subset of Ikonos 2001 Image, (b) Enhanced subset of the Ikonos 2001 Image.

4.4 Principle Component Analysis

The spectral response of the signal from a same location but at different times $T1$ and $T2$ very often represents a linear relation (Richards, 1993; Singh, 1989). Figure 4.2 shows the plots of the spectral signals from a same area at different time $T1$ and $T2$. The PCA technique transforms these spectral values at time $T1$ and $T2$ into a bi-temporal feature space.

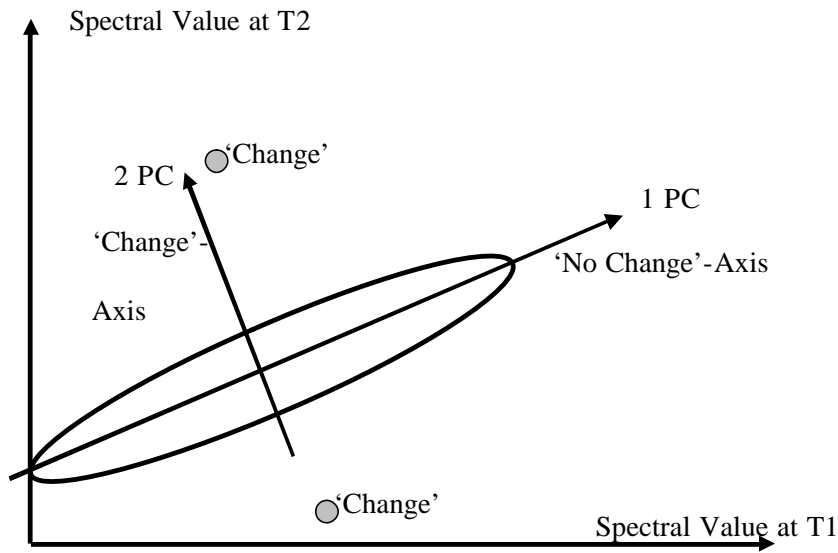


Figure 4.2 Change detection using PCA transformation (Wiemker *et al.*, 1997)

The bi-temporal feature space for a single spectral band i is represented by an element $x_i = [x_i(T_1); x_i(T_2)]^T$, where $x_i(T_1)$ represent the value of pixel 'x' in band i at time T_1 . The unchanged pixels present are linearly linked in the bi-temporal space. They lies in a narrow elongated cluster along the Principal Axis (PC1) (Figure 4.2) (Wiemker *et al.*, 1997). On the other hand, the pixels which have experienced changes in their spectral appearance are expected to lie far away from this axis (Richards, 1993). In other words, the magnitude of 'change' is quantified by the magnitude of the second Principal Component (PC2) given by:

$$C_i = e_{2i}^T (x_i - m_i) \quad (4.1)$$

where e_{2i} is the second eigenvector of the overall covariance matrix C_i (which is 2 X 2 matrix) of the spectral band i . Equation 4.3 defines the covariance matrix:

$$C_i = 1/N \sum (x_i - m_i)(x_i - m_i)^T \quad (4.2)$$

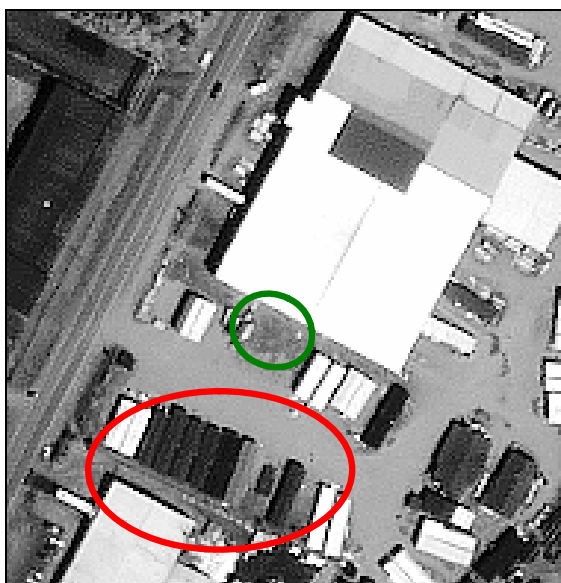
where, $m_i = \frac{1}{N} \sum x_i$ is the mean of all N pixels in that band (Wiemker *et al.*, 1997).

4.4.1 Data Set Used

Two test sites have been selected and are presented in Figure 4.3 and Figure 4.4 for the implementation of the PCA technique. The first test site contains different types of man-made objects such as buildings, roads, parking lot, containers. The second test site Figure 4.4 contains small man-made objects such as cars, huge containers, buildings. Both sites are also characterized by some shadow effects. The objective is to determine the effect of shadows, heterogeneity, and size of the objects on the derived change using the PCA technique.

4.4.2 Implementation of Image to Image Change Detection using PCA

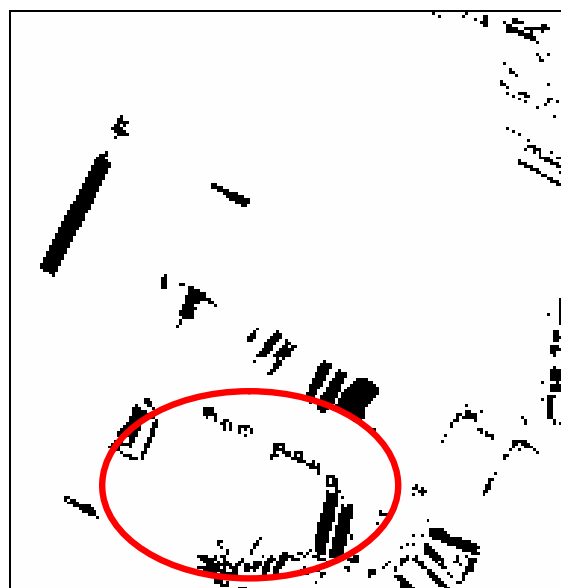
The PCA method is one of the most reliable and accurate traditional change detection methods. The objective of implementation of this method is to determine the feasibility of the method for change detection of man-made objects. The PCA transformation is used to transform the temporal images into parameter space. The magnitude of elements in the parameter space is given by equation 4.1. By applying an appropriate threshold on the magnitude of the elements in the parameter space (equation 4.3), the information about changed elements is derived. To obtain information about the changed pixels one need to do the inverse transformation of derived changed elements into image space.



(a) Ikonos subset of year.2002



(b) Ikonos subset of year 2001

(c) The Change Image obtained using
Threshold 1 = 1.5σ (d) The Change Image obtained using
Threshold = 2σ **Figure 4.3 Change detection using PCA technique (Case Study 1)**

$$T_i = |C_i| - \frac{\sum C_{i(nm)}}{n \times m} < k\mathbf{s} \quad (4.3)$$

In equation 4.3, 'k' is the scale factor, \mathbf{s} is the standard deviation of the $C_{i(nm)}$, which is the magnitude of all elements along PC1.



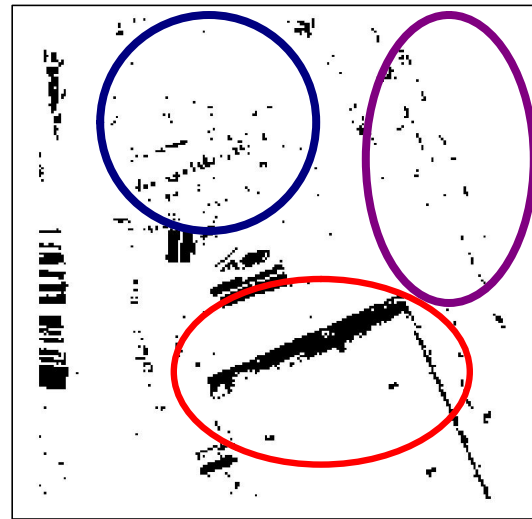
(a) Ikonos subset of year.2002



(b) Ikonos subset of year. 2001



(c) The Change Image obtained using Threshold $1 = 1.5 \sigma$



(d) The Change Image obtained using Threshold $= 2 \sigma$

Figure 4.4 Change detection using PCA technique (Case Study Two)

The selection of the threshold is not well defined. The detection of an appropriate threshold is based on trial and error basis. One needs to vary the scale factor 'k' in equation 4.3 to get an appropriate threshold. Figure 4.3c, d and Figure 4.4c, d present the detection of the changes for two different thresholds for case one and two respectively. The scale factors 'k' for the selected threshold one and threshold two are two constant values, 1.5 and 2.0 respectively. The scale factor represents the diversion of the changed pixel from PC1.

The test site one (Figure 4.3a and b) has been selected to study the effect of the heterogeneity on the change detection derived using PCA. This test site contains heterogeneous man-made objects such as buildings, roads, parking lot, containers. The second test site (Figure 4.4a and b) has been selected to study the effect of the shadows in the image on the change detection derived using PCA. The highlighted portion of Figure 4.4a and b shows shadow of the building located in the central south portion of the test site. The size of the shadows in these images (Figure 4.4a and b) is significant as compared to the object size, as well as it is different due to temporal effect (different sun angle). Thus test site one and two are ideal candidates for the study of effect of heterogeneity and shadows on the change detection respectively.

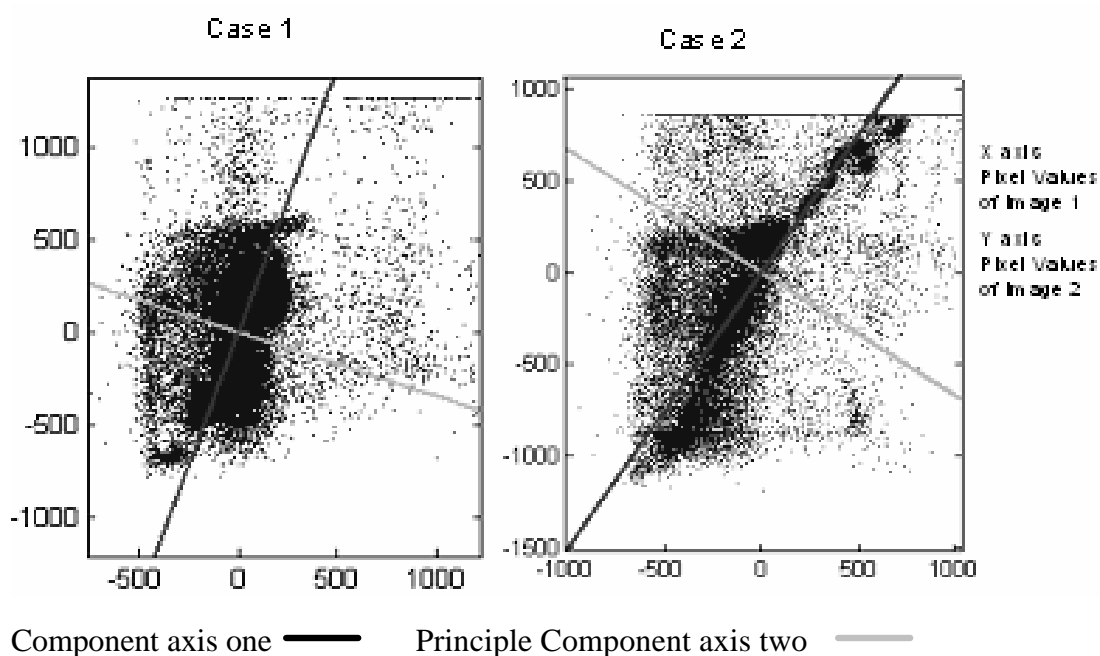


Figure 4.5 Parameter space plot obtained (case study 1 and 2) after the PCA transformation

Figure 4.5 shows the transformed data into the parameter space for the case studies. PC1 and PC2 represent the axes of the parameter space. The PC1 axis is shown in black and PC2 in gray. The unchanged pixels lie along the PC1 axis and those pixels which undergone change appears more diverted from the PC1 axis and lies along the PC2 axis. The left image in Figure 4.5 shows the parameter space for case study one. It can be seen that the PC1 axis is more tilted towards a vertical axis. From the property of the eigen vectors, ideally it should be in the diagonal direction. However, this will only happen if both images are at the same contrast level. In case study one the 2001 and 2002 Ikonos panchromatic images do not have the same contrast level, so the PC1 axis is diverted from a diagonal direction. For case study two, the two input images have similar contrast levels, so PC1 axis is more towards a diagonal direction.

4.4.3 Analysis of the Results Obtained Using PCA Technique

This section examines the ambiguities introduced by different phenomena in the detected change by PCA.

The Effect of Misregistration on the PCA Results:

We can see from the highlighted portion shown by green ellipse in Figure 4.3c, that small misregistration of 0.4 pixels caused a lot of tilted horizontal lines as change in the output change image. These misregistration and difference in shadows appear more predominately at the edges of the objects. This also implies that PCA method is very sensitive to even small change and it is a really efficient technique for the change detection.

The Effect of the Heterogeneity on the PCA Results:

It can be seen in highlighted portion in red ellipse of Figure 4.3a and b that few relatively small dark objects (*i.e.* containers) located at the bottom portion of the images are present in the image of year 2001 but not in the image of 2002. However few new containers in 2002 have replaced the containers from 2001 at that location. This change could not be detected completely using the PCA method due to similar spectral responses of the objects. Only shadows of containers have been detected as change. On the other hand the small objects (containers) highlighted by green ellipse in Figure 4.3b are missing in Figure 4.3a: those objects were not replaced by other objects. This change is detected in the PCA output change image.

The Effect of Shadows on the PCA Results:

One can clearly see in Figure 4.4c and d that the difference in the shadow of the building in the red ellipse has been detected as change. The shadow of the building appeared in the year 2002 is much bigger in size than in year 2001.

The Ability of the PCA Technique for the Detection of the Small Change:

It is also observed from Figure 4.4b that there are many small man-made objects (*i.e.* cars) in the upper portion of the 2002 image (in a blue circle) those are missing in the 2001 image. Even this change is partially detected by the PCA technique. The change in vegetation (in the violet colour) is also detected. This detected change in vegetation is useless for the change detection of man-made objects. This change information is partially eliminated from the results by using a higher threshold *i.e.* 2σ . However this happens at the cost of the loss of some change information of small man-made objects such as cars.

4.4.4 Implementation of Image to GIS Change Detection using Post

Classification Change Detection

The objective of this research is to detect changes in man-made objects such as buildings using VHR remotely sensed images for GIS update. The maximum likelihood supervised classification method helps us to detect the human developed areas. It further classifies the different man-made objects into classes such as roads, buildings and parking areas. This is also helpful for detecting every man-made object. Figure 4.6a presents the

multispectral Ikonos image used for the classification. The supervised classification approach used the training samples shown in Figure 4.6b.

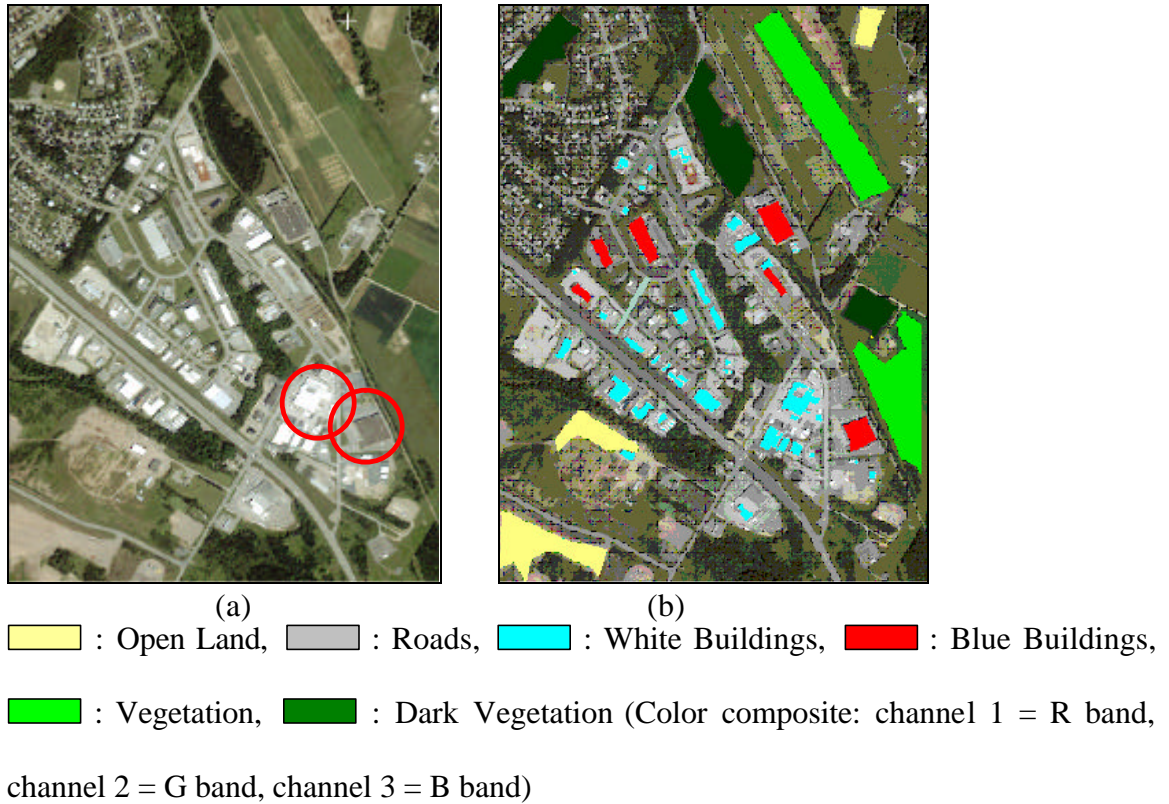


Figure 4.6 (a) Multispectral Ikonos image (b) Training data set used for the classification

The change detection between the multispectral image and the GIS data was carried out using a post supervised classification comparison. The following steps have been applied for detecting the changes.

Step 1: GIS Data set to image conversion

The available NTDB data set is in a geo-referenced shape file format, *i.e.* the GIS data contains information about buildings, build-up areas, roads, highways or railway line in separate shape files. The polygon type of the Building shape file has been selected as input from the GIS data set. The input shape file has been rasterized to a binary image. Figure 4.8a presents the GIS building layer in the rasterized format.

Step 2: Development of separate feature layer images using a supervised classification

The classification process is carried out using the maximum likelihood classifier. The derived classified image is shown in Figure 4.7. The post processing of the classified image provides a binary feature layer image of the buildings. Since every step in the process is self contained, it is simple to implement and to experiment with different algorithms in a specific step without affecting the rest of the workflow. For defining the class information, 'training bitmaps' have been created for each information class. The selection of five classes - White Buildings, Roads, Vegetation, Open Land and other Types of Buildings - has been made. Spectral values are then assigned to the information classes (bitmaps) that have been created for the Building features. The classified image is presented in Figure 4.7a. The pseudo colour schema of the classified image obtained using supervised classification is shown in Figure 4.7b.

Step 3: Change detection

The PCA method was used for change detection. Here the developed binary images were used as the input data set to the PCA method. A second approach for image to GIS data set change detection task would be the new developed feature extraction based method.

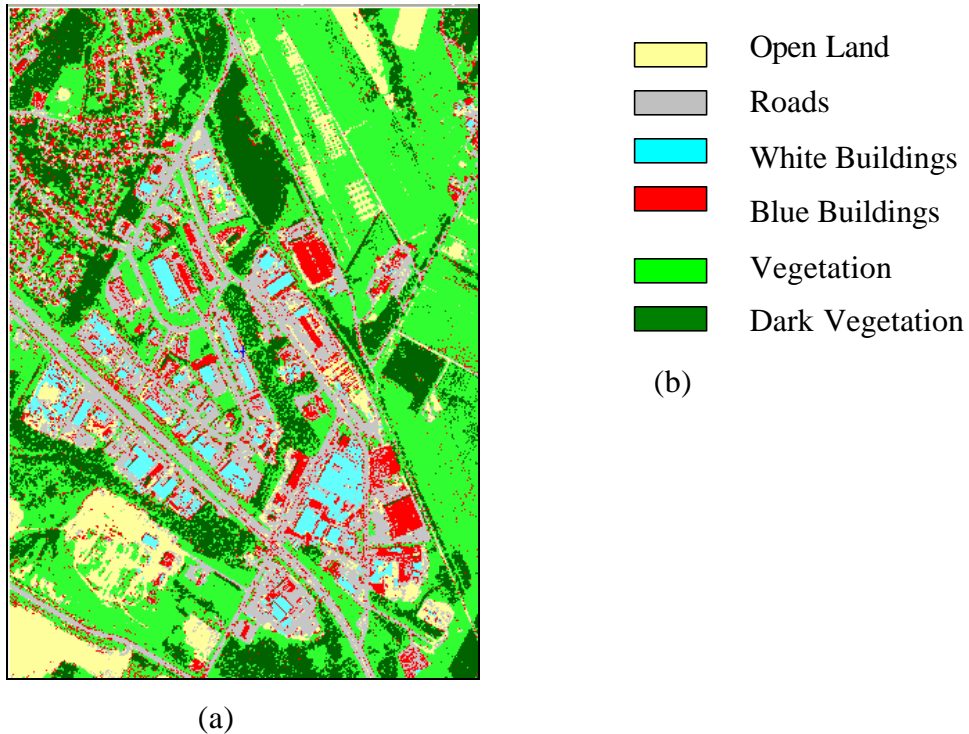


Figure 4.7 (a) Classified Image obtained using supervised classification, (b) Assigned (pseudo) colour schema for the classified image

Table 4.1 Classification accuracy of the classified image derived from the supervised classification

Code	Name	Pixels	Reference					
			20	55	90	150	220	250
20	Open land	3949	94.71	0.03	1.04	2.81	1.32	0.10
55	Dark vegetation	5248	0.02	93.65	4.42	0.61	1.30	0.00
90	Vegetation	8330	0.25	3.34	95.51	0.04	0.86	0.00
150	Road	1998	3.15	0.00	4.75	85.29	6.46	0.35
220	Blue buildings	1992	0.75	0.40	0.50	13.45	62.60	22.29
250	White buildings	2205	0.50	0.18	0.00	2.09	4.49	92.74

4.4.5 Change Detection of Buildings

The classified building layer obtained from the maximum likelihood supervised classification method is compared with the building layer of the GIS data for the change detection. As shown in Figure 4.6a, some of the buildings appear in a brownish gray colour, whereas others appear in white colour. Hence buildings are categorized into two classes: White Buildings and Other Buildings classes. A separate bitmap training data set is selected for the classification. When buildings are small it is difficult to extract the exact boundaries of the buildings using a classification algorithm. Errors in the extracted boundaries of buildings appear as change. It is also observed that the misclassification of

buildings as road, open land, parking lots, or others, caused more errors in the change detection. Table 4.1 shows that the classification accuracy for the blue building layer is only of 62.6 percent. Even though some of the changed buildings are very well detected by this approach, most of the detected changes have been found false.

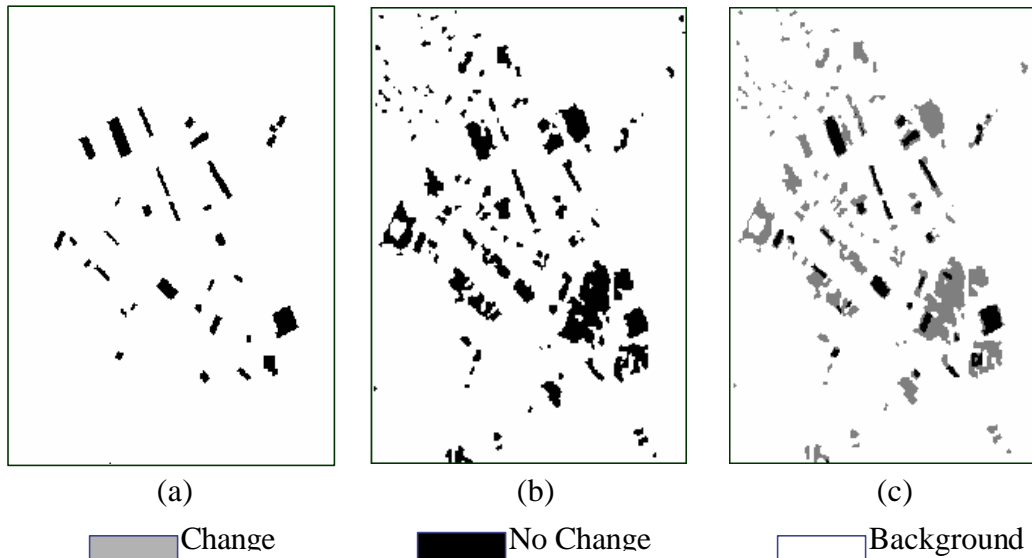


Figure 4.8 (a) Building layer of NTDB data set, (b) Derived building layer using classification (c) Derived change between GIS building layer and classified image building layer using PCA technique

4.5 Limitations of the Traditional Change Detection Method

After the analysis of the two traditional methods for the data sets, it is found that they have limitations for change detection. The supervised classification method is inaccurate for the classification of urban areas due to presence of heterogeneous objects with similar spectral response properties which leads to misclassify the objects. It is thus unreliable for the change detection. Traditional methods are inaccurate and their results are dependent on the registration accuracy. Small misregistration causes error in the detected

change (Radke *et al.*, 2005). These methods are not suitable in urban areas where heterogeneous types of objects are present. The heterogeneity introduces more chances of misclassification. The PCA method does not categorize the detected changes according to the type of objects. This method just defines the overall changed pixels in the image. Hence, this method is not very useful for detecting temporal changes in urban man-made objects. Supervised classification method is semi-automated and needs an accurate training bit-map for the classification. The post-classification and PCA methods are not able to categorize the results into missing objects, unchanged objects, newly emerged objects.

Most of the man-made objects have well defined shapes and sizes. That information is certainly helpful for change detection. These two methods take only the information about the spectral reflectance of the objects and do not consider any other properties of the objects such as shape and size for change detection. These methods don't specify change corresponding to man-made objects such as buildings. The change information obtained using these methods are not very useful for the GIS updates due to incompatibility.

Chapter 5

Automated Building Extraction Based Change Detection

5.1 Introduction

This chapter proposes and investigates the newly developed method for detailed change detection. As mentioned earlier, the main objective of this research is to detect the changes in man-made objects for automating GIS updates. GIS broadly categorizes man-made objects into two types such as: a poly-line type and a polygon type features. Man-made objects such as roads, railway tracks, or pipelines are considered as poly-line type and buildings or parking lots as polygon type. However, remotely sensed images are not useful for the detection of underground objects such as pipelines. For simplicity at this stage, all poly-line type objects are considered as roads and all polygon type objects as building. So, man-made objects are broadly divided into two categories such as: roads and buildings. The extraction of one type of man-made objects leads to a helpful information for the extraction of the other type. For example buildings extracted can be excluded from the extraction of roads: this partially increases the accuracy and efficiency of the road extraction process and vice versa.

The extraction of buildings from VHR images is a challenging task due to heterogeneous surroundings. For an accurate extraction of buildings, one needs very high resolution images and/or three dimensional data such as LIDAR (Light Detection and Ranging). This research only deals with the 2-D VHR imagery for the extraction of buildings. Presently, there is no automated reliable method available for this kind of

extraction. Thus, this research attempts to develop a new automated method for building extraction and change detection.

5.2 Need for the Feature Extraction Based Technique

The necessity to develop a new method for the extraction of building arises due to the following reasons:

There is no reliable and automated existing method available for building extraction. As seen in the previous chapter, available change detection technique does not detect changes of individual man-made objects.

The extracted features from temporal data sets are useful for detecting the changes of individual objects. For most of the buildings, their boundaries can be reconstructed using few basic shapes such as a 'L' shape corner or straight lines. Hence it is possible to develop a sequential process for building extraction.

An accurate extraction of the object of interest is very essential for change detection. The detection of accurate edges for all features is a very difficult task (Guennadi and Yerach, 2003). The presented newly developed method is based on a feature extraction using multiple edge detected images based on different edge detecting operators. The advantage of developed method is that if a part of the feature is not detected in one edge-detected image, it can be reconstructed using the other edge-detected images.

5.3 Frame Work for the ‘L’ Shape Template Matching Automated Building Extraction Technique

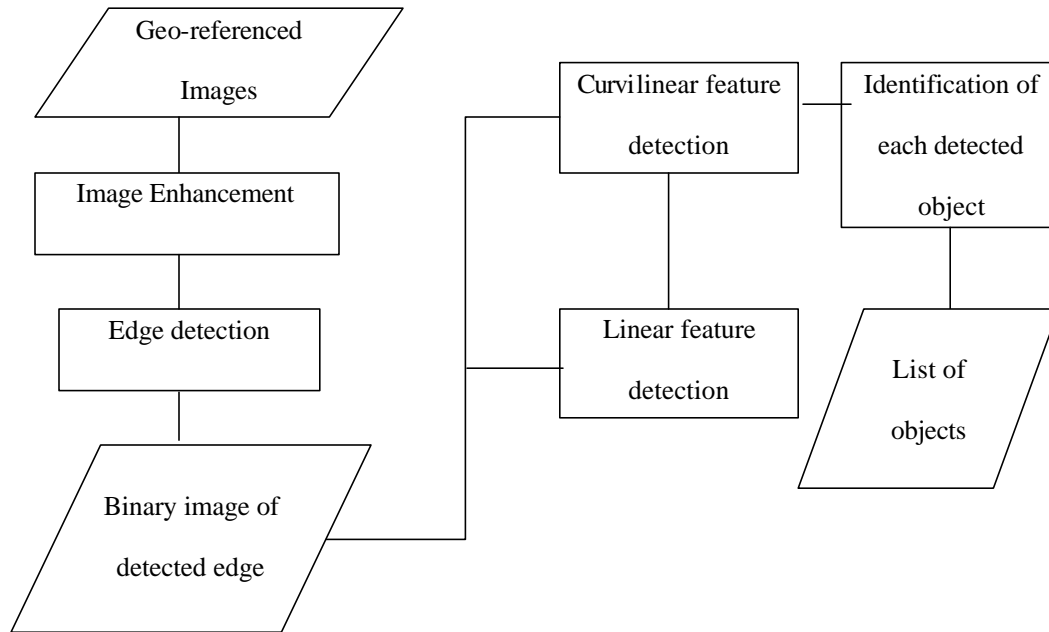


Figure 5.1 Frame work for the Building extraction

The author used PCI Geomatica software for the implementation of image enhancement and edge detection. The developed programs have been implemented using Matlab 6.5 for linear and curvilinear feature extraction, assignment of identification value to extracted features, and change detection.

Figure 5.1 presents the frame work for the newly developed ‘L’ shape template matching building extraction process and each step is detailed in the following sections.

5.3.1 Geo-Referencing and Image Enhancement

Geo-referenced data is essential for accurate change detection. The 2001 and 2002 Ikonos panchromatic images are used for building extraction. These images are orthorectified with the precision of 0.9-2.0 metres (Wang and Ellis, 2005). Only an image enhancement is needed for a better edge detection.

5.3.2 Edge Detection

The Sobel edge detection operator (Sobel, 1990) as a first order derivative type operator gives thick edges at the locations of edges in the image. The Laplacian type 2 edge detector operator (Gonzalez and Woods, 2001) is a second order edge detector and gives thin edges. Both types of edge detectors are used to get maximum information about the edges of the objects. The thin edge-detected image is used for extracting preliminary building boundaries. The missing edges in the preliminary extraction process are then detected from the thick edge-detected image. The detected edges are converted into a binary format using an appropriate threshold. The selection of the threshold is not a standardized process. One needs to adopt trial and error approach for the detection of the appropriate threshold for the conversion of the edge detected image into a binary image of boundaries. The selection of a high threshold eliminates many edges from the edge detected image. A low threshold value leads to noise in the derived binary images. Noisy pixels may appear because of shadow effects or presence of trees. These noisy pixels appear in the form of non-sharp edges. Thus by selecting appropriate threshold one can eliminate those unwanted edges.

5.3.3 Linear Feature Extraction

The boundaries of most of the buildings can be represented using corner points and lines connecting those corner points. The following steps have been applied for the building extraction process using VHR image.

Step 1: The corner points of the objects are considered as a starting point for the extraction of the buildings. In this step, corner points in the binary edge-detected image are detected using the Forstner operator (Forstner and Gulch, 1987).

Step 2: In this step, pixels of edges of the 'L' shape template are matched with edge detected image at each corner point of the linear objects to find the location and direction of gradient of the edges of it with respect to the corner point. As shown in Figure 5.2, the corner point of the 'L' shape template is kept on each detected corner point. The 'L' shape template is rotated over the edge detected image at an increment rate of 1 degree. The 'L' shape template perfectly matches at the edges of corners of rectangular building. The matched position gives the direction of the gradient of the edges. In case of too many closely located man-made objects the template partially matches at multiple locations thus it is necessary to select appropriate size 'L' shape template and best matched position is consider as position of edges of rectangular man-made objects. This process is repeated at each detected corner point in the binary edge detected image. It is also necessary select best matched position for the detection of position of the corner edges of the rectangular man-made object. The position of non-rectangular objects with straight edges is determined using straight line template instead of 'L' shape template matching. Possibility of detection correct position of corner edges in these cases reduces when

edges of man-made object are not well defined. Detection of the accurate corner point is also crucial as 'L' shape template is rotated around the corner point as shown in Figure 5.2.

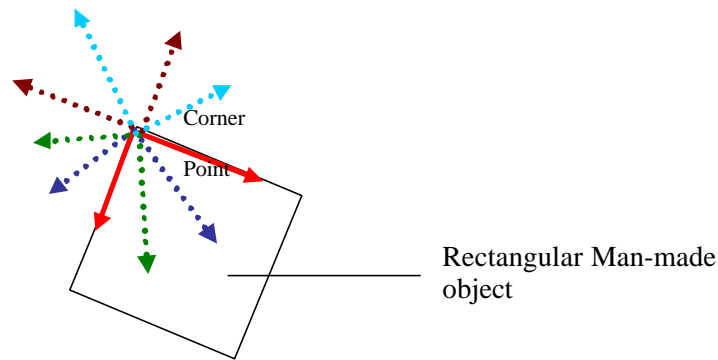


Figure 5.2 Corner point detection using 'L' shape template matching

Step 3: After determining the direction of the gradient of the edges, a line template is used for complete edge detection. The starting point of the straight line template is the corner point. This straight line is matched with the edge detected binary image along the direction of the edge gradient. The process of the straight line template matching is carried out until the line is connected with the other corner point or with the end point of the edge along the direction of the edge gradient.

Step 4: In this step missing edge pixels are programmatically derived. Most of the edges of the objects are found to be discontinuous. It is then necessary to find the missing pixels of the edges. As shown in Figure 5.3, the neighbouring pixel of the missing edge pixel is always found to be an end pixel of the detected edge. To detect the missing pixels of the edge, the line template is further extended by four pixels starting from the end point along the direction of the gradient of the edge. If at least two out of the four pixels of the

extended line template match with the edge detected image then the two other pixels are considered as missing pixels. These detected missing edge pixels are assigned with a high gray level value. Sometimes this step introduces spurious pixels as missing edge pixels. It may lead to the connection of two separate objects.

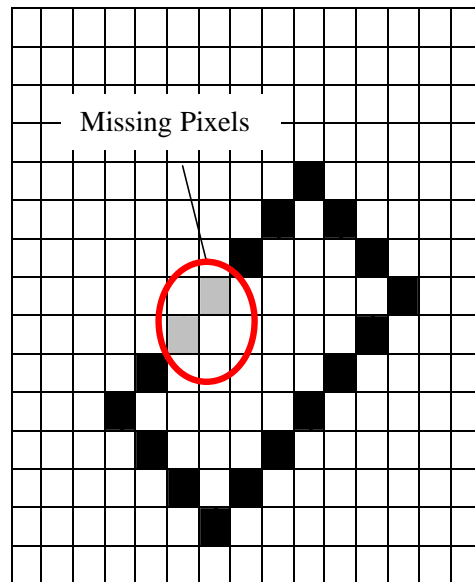


Figure 5.3 Missing pixels in the object

Step 5: It is necessary to identify each building as a separate object. The buildings are of polygon type and the edges corresponding to a building's boundaries form a closed loop. The boundary of linear rectangular buildings can be then defined as an isolated group of pixels connecting the corner points and forming a closed loop. All linear shaped buildings are extracted based on this condition.

The steps 1 to 5 are used for the preliminary building boundary extraction. It is observed that most of the extracted boundaries of the buildings are incomplete as seen in Figure 5.6c and d. These missing edges are then obtained using the thick edge detected

image. Most of the edges are very well detected in the thick edge image. The positional information of the preliminary detected buildings is used to obtain the information about the missing portion of the extracted boundaries of the buildings at preliminary feature extraction step.

To detect the missing edges from the preliminary stage, the positional information of the end pixels of the edges derived in this stage is used along with the thick edge image. The algorithm checks if there is any edge between these end points in the thick edge image. If there is an edge, the missing edge pixels are detected.

5.3.4 Curvilinear Feature Extraction

The curvilinear buildings are those which do not have all sharp corners. Man-made object shown in Figure 5.4 appeared to be curvilinear due to shadow effects and illumination condition. Extraction of such curvilinear buildings is a challenging task due to the absence of corner points and direction of edge gradient to trace the object boundaries. In this case, the start point of the feature extraction process is the nearest pixel to the feature from the image origin. Processing the 'L' shape matching is not possible in this case. The groups of pixels corresponding to the boundary of the buildings are detected only on the basis of their connectivity. Most of the times these types of buildings are found to be partially linear (Figure 5.4), so parts of the object are detected using the process of linear object extraction. The rest of the boundary is detected based on the connectivity and formation of a closed loop by this group of pixels. The highlighted object from Figure 5.4 is successfully extracted using 'L' shape template matching technique (Figure 5.7b). In this case study there is no actual curvilinear feature. However, the discussed example

shows the ability of the developed 'L' shape template matching method for the extraction of curvilinear objects.

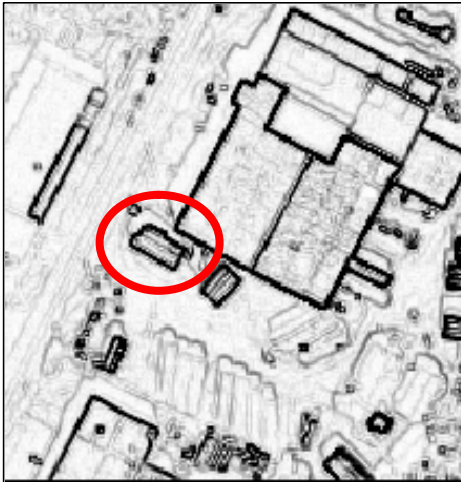


Figure 5.4 Example of semi-curvilinear feature

5.3.5 Identification of the Extracted Objects

The extracted objects (buildings) have been assigned unique identity values for the identification purpose. Each extracted building boundary is observed as a connected separate group of pixels. However, groups of pixels corresponding to different objects do not have any adjacency among them.

5.3.6 Listing of the Extracted Objects

Finally the extracted objects have been listed. This step is necessary for the recognition of their counter part of extracted objects from the other temporal image. Processing the list of the objects consists of the detection of the location and the identification value of the detected object from both temporal images. The same identification value has been

assigned to same object located at same location. All the polygon types of the extracted objects were considered for the listing.

5.4 Results of Change Detection Based On Automated Building Extraction Process

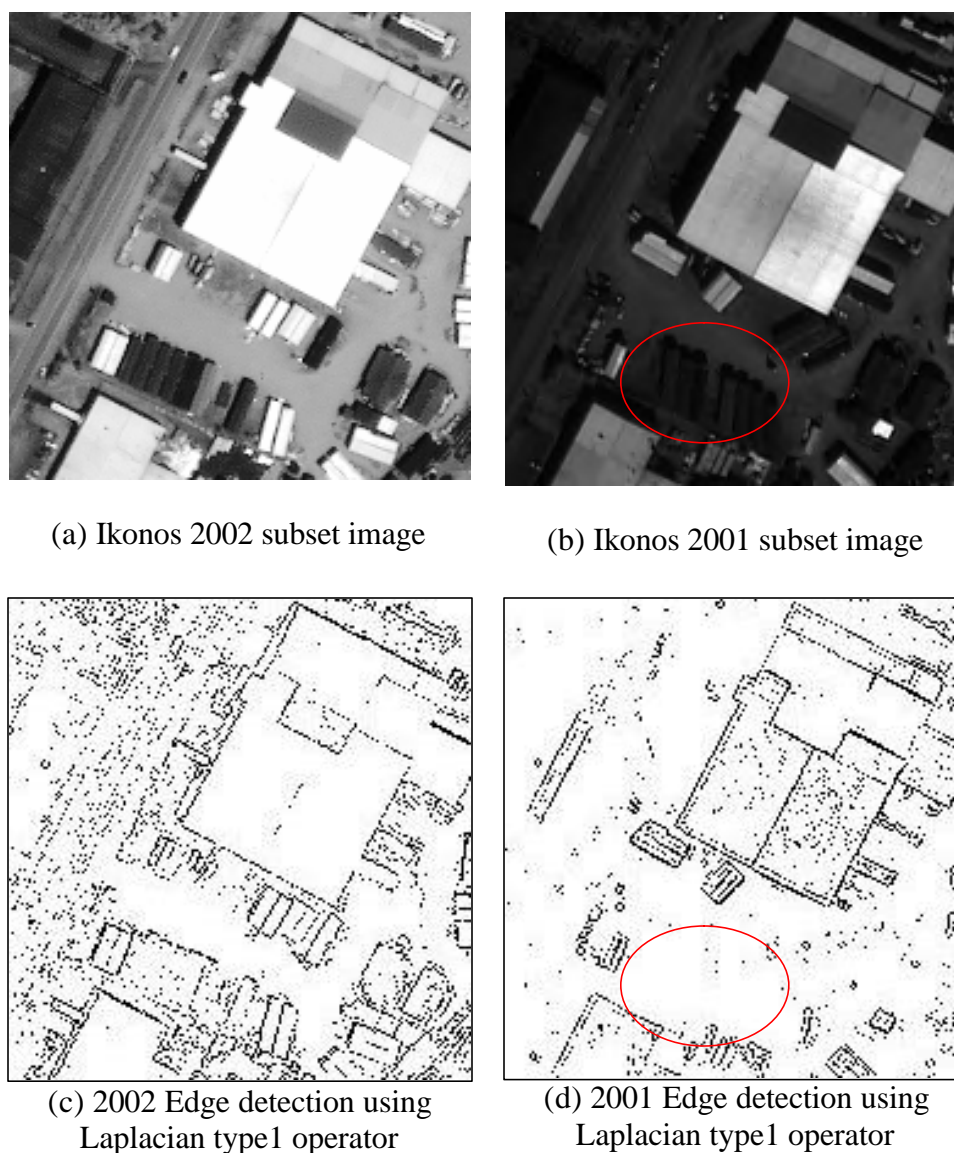
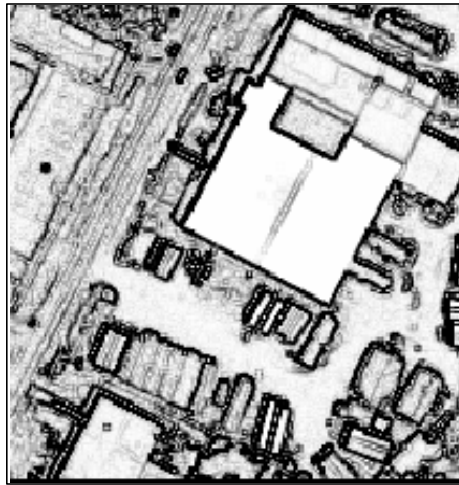


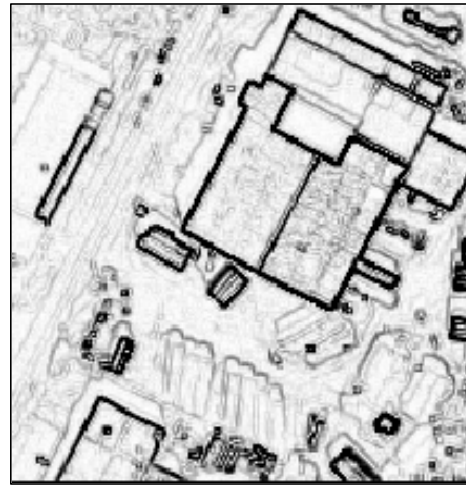
Figure 5.5 Input images used for extraction of buildings

Figure 5.5a and b are enhanced subset images of the Ikonos panchromatic data set. Figure 5.5c and b presents the corresponding edge detected images obtained using the Laplacian type 1 operator. It can be clearly observed that the contrast in the 2002 image is better, which means that in the corresponding edge detected image, most of the edges appear sharply but at the cost of additional noise. The 2001 image is of poor contrast; this explains why some of the edges of few small objects contain in the red ellipse in Figure 5.5d are missing in the corresponding edge detected image. However the 2001 edge detected image contains less noise. When adjusting the contrast of images for better edge detection, one need to decide the optimal trade-off between details of the edges needed and noise introduced in the edge extracted image. Finally using an optimum threshold we convert these edge detected images into binary edge images. The optimum threshold is selected on a trial and error basis.

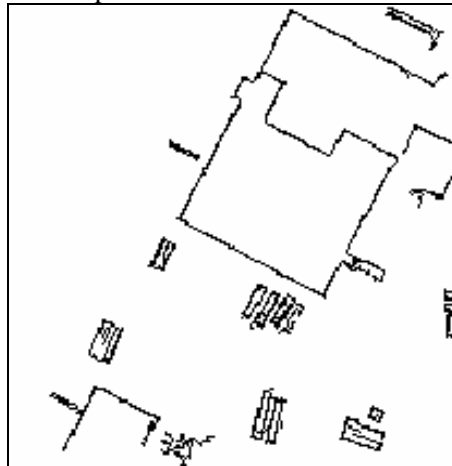
Figure 5.6a and b show the edge detected images obtained using the Sobel operator. These images are used for determining the missing edges of the extracted objects Figure 5.5c and d. It is not possible to use this edge detected images in the first stage, as a line-following algorithm has been used for the boundary detection based on thin edges. Figure 5.6c and b shows the final extracted boundaries of the objects at the end of the first stage. Figure 5.7a and b present the modified extracted objects. It is obtained at step 5 of o linear feature extraction.



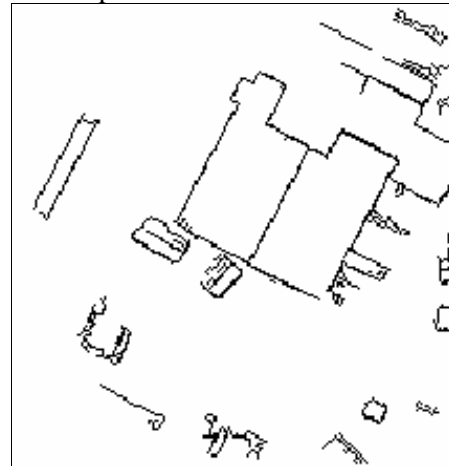
(a) Edge detection using Sobel operator



(b) Edge detection using Sobel operator



(c) Preliminary extracted objects from 2002 image



(d) Preliminary extracted objects from 2001 image

Figure 5.6 Second stage input images to obtain modified object boundaries

The missing edge pixels are detected using information from the thick edge detected image at this step. Thus this step modifies the preliminary extracted objects into a more complete form. It can be clearly seen that some of the edges of the detected objects which are not determined in the first stage (Figure 5.6c and Figure 5.6d) are detected at this stage as seen in the highlighted portion of Figure 5.7a and Figure 5.7b.

The extraction of a complete object is very essential for GIS update. Figure 5.7c and d show the changed objects. The boundary pixel matching of the same object in both temporal images Figure 5.7a and b provides us with the changes that have occurred. Boundary pixel matching used the positional information and the assigned identification values of the extracted objects. The boundary pixels of the same object in both extracted images are compared. The boundary pixels of the objects from Figure 5.7a are considered as reference and that from Figure 5.7b are compared with the reference. Ideally each boundary pixel of the extracted object should have its representation in both extracted images at the same location. It is observed that only 35 percent of the boundary pixels of the extracted objects fulfilled this criterion. But 35 percent of pixels were found offside by only 1 pixel. This happens due to effects of small misregistration, shadow effects, false representation of missing pixels and false detection of edge gradient. Therefore to consider this offset of 1 pixel, instead of a direct pixel by pixel matching, we applied a search window of a 3 X 3 size. For each boundary pixel matching from Figure 5.7a into Figure 5.7b, a 3 X 3 search window with the center located at the pixel of interest in Figure 5.7b is used. If the number of matched pixels is greater than 70 percent of the total boundary pixels of the object, it is considered as an unchanged object. If it is less than 30 percent then the object is considered as a changed object. Thus based on these criteria all extracted objects were categorized as changed or unchanged objects. The newly developed method can not detect partially changed objects as it is difficult to find if the changed pixels are due to an actual change or due to misregistration, shadow effect or missing edges. However it is observed that spurious classification of changed pixels as unchanged and vice versa makes it difficult to detect partial changes. But it is observed in

the case study that these effects are less than 30 percent of the total boundary pixels of the objects. Figure 5.7c and d presents the missing man-made objects (buildings and huge vehicles) from one image but which are present in the other image.

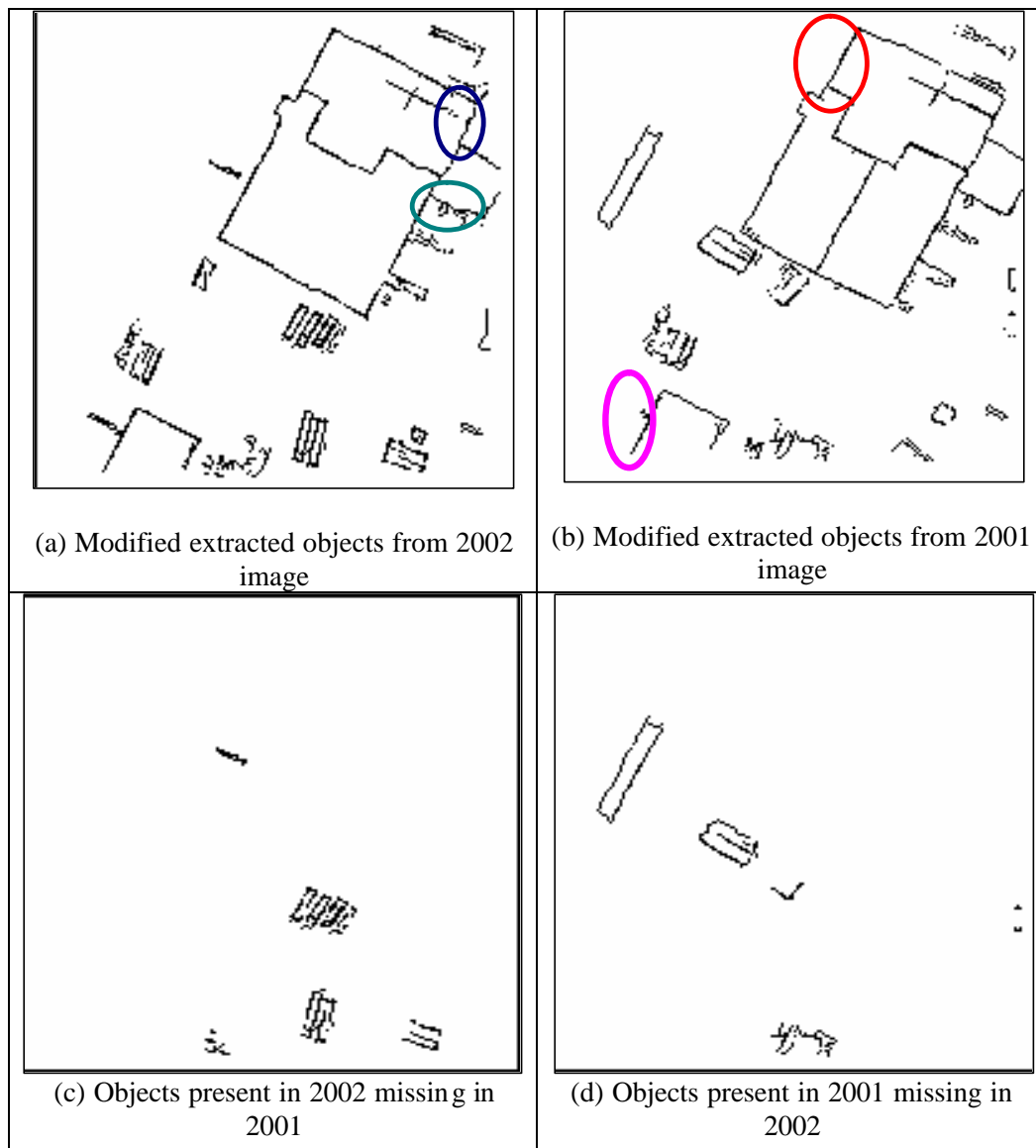


Figure 5.7 Final results of the automated building extraction process

5.5 Implementation of the 'L' Shape Template Matching Method on the Blue Band of the Fused Image

The spectral responses of man-made objects are high in the Blue band (0.45 to 0.55 μm) of multispectral images which improves contrast (Horne, 2003). To obtain better information of the building boundaries the author implemented the developed 'L' shape template method on the blue band of the IKONOS multispectral image. The spatial resolution of a multispectral Ikonos image is four metres on the other hand the spatial resolution of the Ikonos Panchromatic images is one metre which is found suitable for building extraction. The boundaries of small objects such as buildings are not very well defined in the multispectral image as seen in the (Figure 5.8 a) due to a poorer resolution. Data fusion is necessary to obtain data with very high spectral and spatial information. The Intensity Hue Saturation (IHS) technique is used for the data fusion (Meenakshisundaram and Couloigner, 2004). A data fusion process provided a new image with three spectral bands at one meter spatial resolution. The classification of the fused images should give more accurate classification results due to a higher spatial resolution and a better contrast. Details of the IHS techniques for the data fusion are given in chapter 3.



(a) Multispectral Ikonos 2002 image



(b) Multispectral Ikonos 2001 image



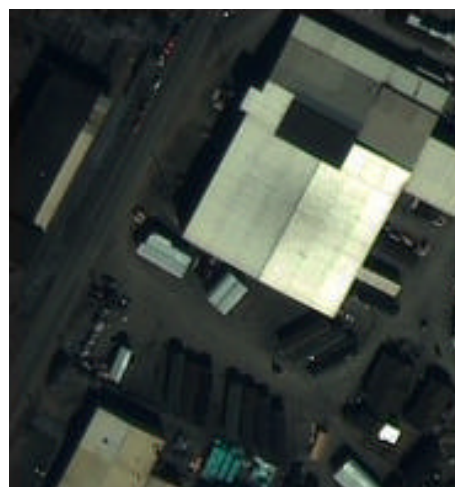
(c) Panchromatic Ikonos 2002 image



(d) Panchromatic Ikonos 2001 image



(e) Pan-sharpened Image of year 2002



(f) Pan-sharpened Image of year 2001

Figure 5.8 Pan-sharpening via the IHS technique

All images shown in the left side of Figure 5.8 are of year 2002 and all images shown in the right side are of year 2001. The images shown in second row are Ikonos Panchromatic images and in the first row are the multispectral images of Ikonos. The heterogeneous objects such as buildings, roads, big size containers, and shadows, are present in the test area as seen in Figure 5.8. The spatial resolution of multispectral images is 4 m which is not sufficient to clearly identify these heterogeneous objects (Figure 5.8a and b). On the other hand these objects are very well defined in the panchromatic images (Figure 5.8c and d) due to its higher spatial resolution (1 metre). These two types of images are used as input for the data fusion. Figure 5.8e and f shows the derived fused image provided by the IHS data fusion. The fused image obtained is of one meter spatial resolution. Thus one can clearly identify man-made objects such as buildings and large size containers in the fused image which was difficult in the original multispectral image.



(a) Blue band of the fused 2002 image



(b) Blue band of the fused 2001 image

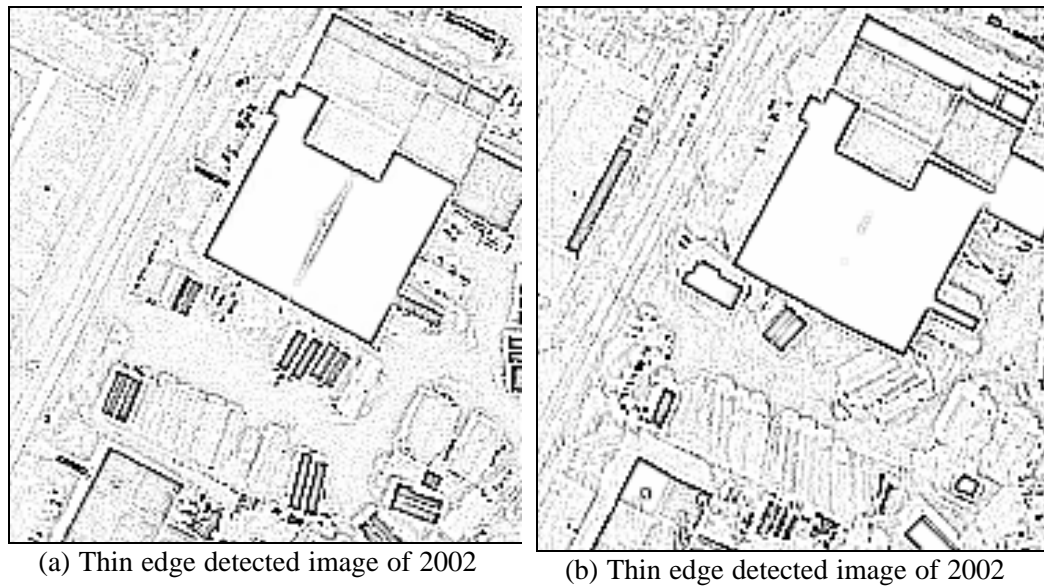
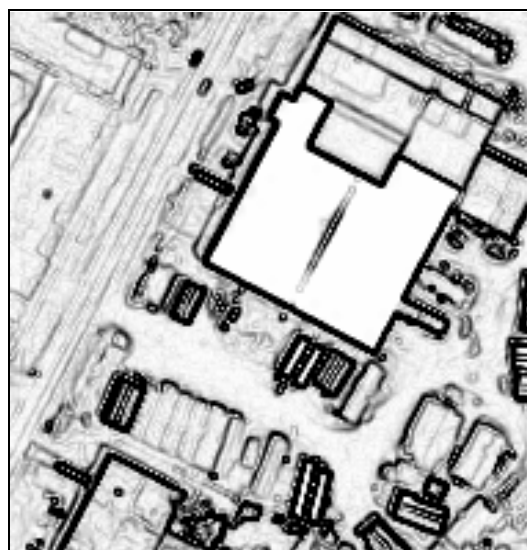
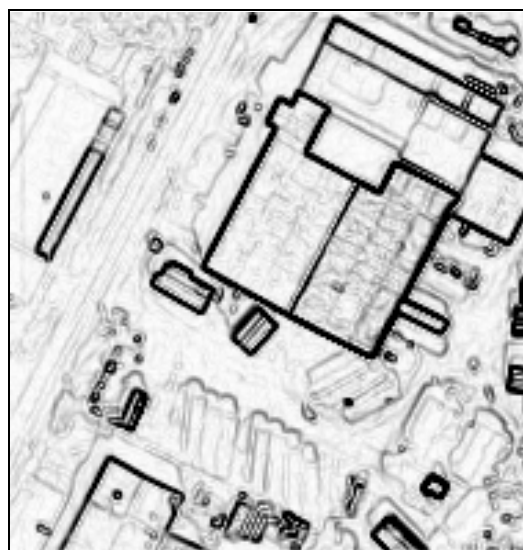


Figure 5.9 Input images used for extraction of buildings using Blue band of fused images obtained using IHS technique

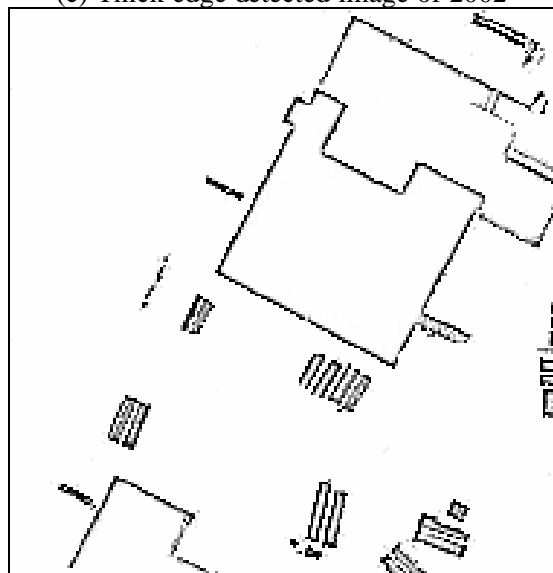
Figure 5.9a and b show the enhanced Blue band of the fused image of year 2002 and 2001 respectively. The enhancement of the image is carried using histogram equalization. These enhanced images are used for the edge detection. The Laplacian type 1 operator is applied to obtain the thin edges (Figure 5.9c and d). These images are used for the preliminary extraction of man-made objects such as buildings. The preliminary feature extraction is carried out as discussed in the section 5.3.3 and 5.3.4. The preliminary extracted objects from the fused Blue band of year 2002 and 2001 are presented in Figure 5.10c and d. The missing edges of the preliminary extracted objects are derived using the thick edge images obtained using the Sobel operator. Figure 5.10a and b are the thick edges obtained using the Sobel edge detector.



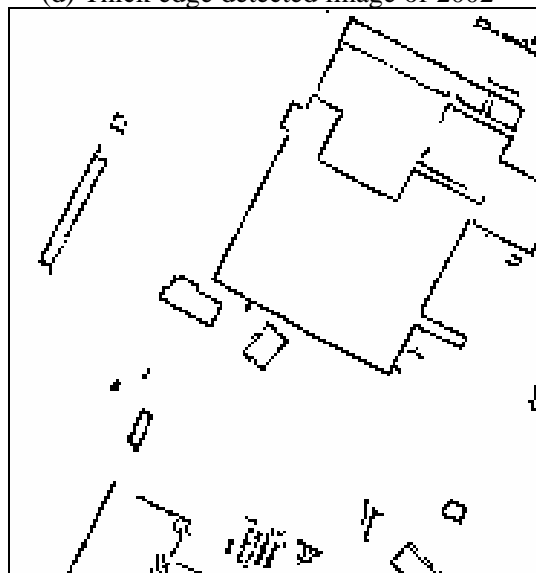
(c) Thick edge detected image of 2002



(d) Thick edge detected image of 2002

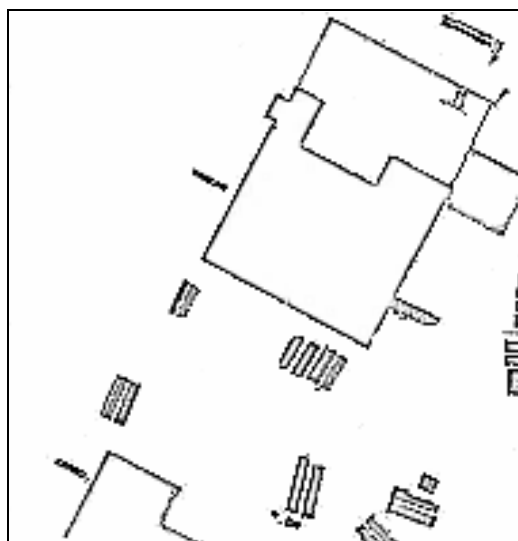


(a) Preliminary extracted objects from blue band of fused image of 2002

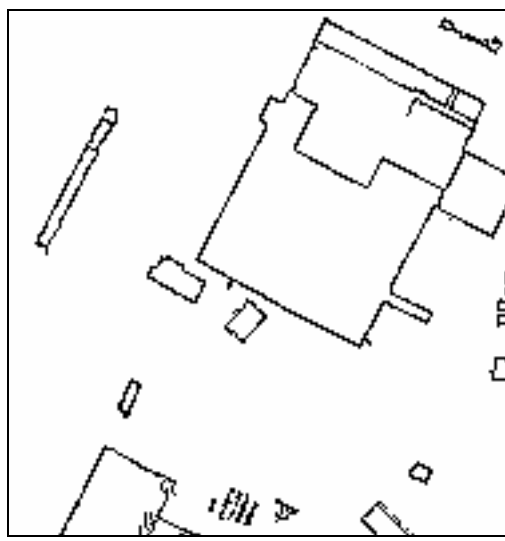


(b) Preliminary extracted objects from blue band of fused image of 2001

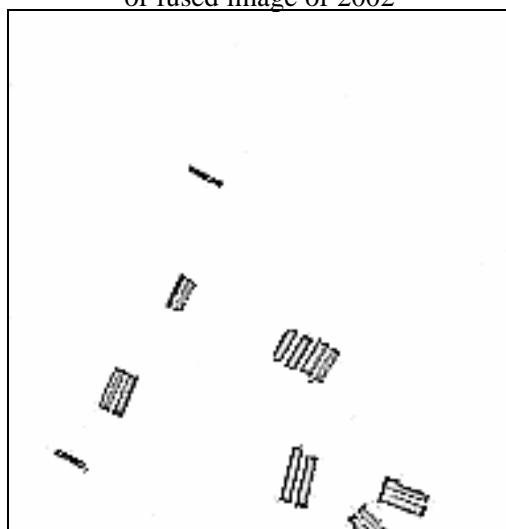
Figure 5.10 Second stage input images to obtain modified object boundaries for change detection of man-made object using the blue band of the fused images



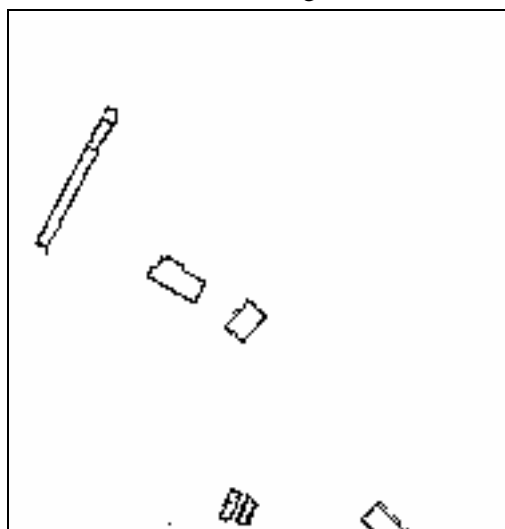
(c) Modified extracted objects from blue band of fused image of 2002



(d) Modified extracted objects from blue band of fused image of 2002



(c) Objects present in 2002 missing in 2001



(d) Objects present in 2001 missing in 2002

Figure 5.11 Final results of the automated building extraction process using the blue band of the fused images

The modified objects obtained by adding the missing edges pixels in the preliminary extracted objects are presented in Figure 5.11a and b. Finally the information about the completely changed objects as discussed in the section 5.4 is extracted. The (Figure 5.11 c and d) show the completely changed objects.

5.5.1 Analysis of the Derived Change using the Pan-sharpened Blue Band

The completely changed objects derived using the fused Blue band are more numerous compared to that obtained using panchromatic image (Figure 5.11 c and d). The thin and thick edge detected images obtained from the fused Blue band image are sharper than those obtained from the panchromatic images. The small object located very close to the big white building is successfully extracted as a separate object. This object in the green ellipse in Figure 5.6 was detected as a part of the big object as they got connected when the 'L' shape template matching technique was implemented on the panchromatic image. The detected changed objects are well defined and are in a more complete form compared to those changed objects obtained using panchromatic images.

5.6 Requirements for the 'L' Shape Template Matching Technique

The 'L' shape template matching technique needs orthorectified images for its successful implementation for the building extraction and change detection. The spatial resolution of the image needs to be less than 2 m for an accurate extraction of the boundaries of the buildings. At this stage this method needs same spatial resolution temporal images for the change detection.

5.7 Observations

An accurate extraction of buildings and other similar shaped man-made objects depends on the clarity of the edges in the edge detected image. Small objects closer to other big objects have been connected in the process of feature extraction using 'L' shape template

matching algorithm and hence it considered both objects as one single object. Even in the modified object images (Figure 5.7a and b), small portions of boundaries are discontinuous but it is still sufficient for change detection. Partial small change in the objects is ignored because of the chosen threshold. It is also observed that most of the changes occurring in man-made objects are very well defined in the changed image (Figure 5.7c and d). The newly developed method can detect temporal characteristic of the changes. The temporal characteristics specify if the change is due to the emergence of new objects or the removal of existing ones. The derived change using this method is compatible for GIS update. Finally the fused blue band found more suitable than panchromatic image for man-made object extraction and change detection as due better clarity of the edges.

Chapter 6

Comparison of the Implemented Change Detection Methods

This chapter examines the results obtained using the PCA, Post-classification and 'L' shape template matching method for the change detection of man-made objects such as buildings. It has been observed that each implemented methods has pros and cons. A comparison of these methods is essential for the evolution of the developed methods into an ideal change detection technique.

6.1 Qualitative Comparison of the Implemented Methods

A qualitative comparison consists of a visual inspection of the change detection results obtained using the different implemented change detection techniques as discussed in Chapter 4 and 5. The following observations are made based on these results:

6.1.1 Change Detection using Supervised Classification

The Supervised classification method has the ability to distinguish the object of interest from the rest of the objects in the image. This method can classify different types of objects in separate classes and forms separate layers corresponding to certain type of objects. The post supervised classification method detects the changes in the object of interest and is useful for preliminary change detection. However this method is unable to accurately define the boundaries of the buildings due to misclassification of parking lots and roads as buildings and visa versa.

6.1.2 Change Detection using PCA

This method provided accurate information about the changed pixels. PCA is a semi-automated method and only needs to adjust the threshold to discriminate the changed pixels from the unchanged pixels as explained in chapter 4.

However, the change detection obtained using PCA depends on the image enhancement and the radiometric adjustments applied. The changed image obtained using the PCA method contains more noisy pixels because PCA is based on the radiometric values of the pixels in the image. Shadow effects appeared as change in the PCA results which is not observed in the results from the 'L' shape template matching based method. Sub-pixel level misregistration caused errors in the change image derived by the PCA method. The PCA method provides the overall changed pixels but does not discriminate missing objects from newly emerged objects.

6.1.3 Change Detection using 'L' Shape Template Matching

The 'L' shape template matching technique has the ability to discriminate newly constructed objects from missing objects. The results obtained from this method are in a binary format and compatible for GIS update. This is a semi-automated method useful for the extraction and the change detection of large size containers and vehicles. The performance of 'L' shape template matching technique can be improved using fused Blue band as observed in the chapter 5 because all features in it appeared clear and sharper.

However, the precision of the derived results using the 'L' shape template matching method depends on the clarity of the detected edges. This method can not

discriminate the buildings from other polygon type objects, such as containers or vehicles.

6.2 Quantitative Comparison

Quantitative comparison is a difficult task as the result obtained using change detection techniques vary from case to case. For example, the results may vary with the heterogeneity of the location, the density of the objects present in the image, the presence of shadows, the occlusion of the objects of interest and the types of the other objects present in the images. The process of comparison needs to be generalized. The comparison with ground truth is a perfect way of evaluating the accuracy of automated change detection. However, to obtain ground truth information is infeasible. The ground truth information can be in the form of: location of the changed objects, the nature of the change in the object that is if the change is partial or complete, whether the changed objects have been replaced by new objects or renewed, geophysical information: size, shape and location of the eliminated, replaced or newly constructed objects. To obtain this information one needs to carry out field survey, which is very time consuming and expensive.

A quantitative comparison of the implemented change detection methods has been performed, without considering the ground truth. A manual digitization process is used for the detection of actual number of changed and unchanged pixels which are then considered as reference (Figure 6.1). Table 6.1 presents the results of the quantitative comparison.

Table 6.1 Quantitative comparison of the implemented change detection techniques

	Matched Pixels	No of Changed Pixels	No of Misclassified changed pixels	Percentage of misclassified pixels = (Misclassified pixels/ Reference Matched Pixels)
Digitization (Reference)	19837	1786	0	0
PCA	82.8%	4390	2604	13.1
Post Classification	68.3%	5312	3526	17.8
'L' Shape template matching using Panchromatic Image	90.3%	1231	555	3
'L' Shape template matching using Pan-sharpened Blue band	96.1%	1489	243	1.22

The quantitative comparison is based on the results obtained by the implemented methods for case study one. The boundaries of every unchanged and changed buildings present in the Ikonos Panchromatic subsets have been manually traced (Figure 6.1). A specific colour which is blue and red is assigned to the traced unchanged (blue) and changed (red) boundaries for identification purpose. The total numbers of changed and unchanged pixels of the assigned colours are programmatically counted. This is done for both the 2001 and 2002 panchromatic image subsets. The total number of the change pixels from each subset is added to obtain the total number of the changed pixels for reference.

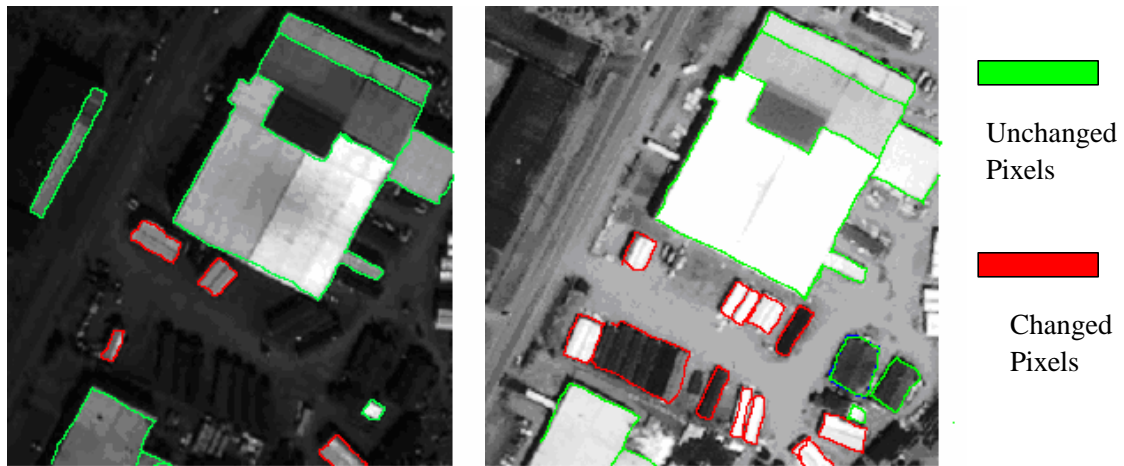


Figure 6.1 Digitized reference images for change detection

The ‘L’ shape template matching method is also based on the edge detection of buildings and hence direct comparison of the results obtained is possible. The PCA and post supervised classification method detect complete changed portion of the feature and not only the boundary pixels. In these cases the edges of the derived changed and unchanged objects are detected for the quantitative comparison. The PCA technique detects overall changed pixels and does not further categorize the change based on the objects. This leads to more misclassified changed pixels for the PCA method (thirteen percent). For the post supervised classification technique, misclassification leads to poor accuracies. It is observed that the developed ‘L’ shape template matching has a better accuracy (90.3 and 96.1 percent) in detecting the total number of matched pixels of the buildings whereas the accuracy of the supervised classification and PCA techniques is only 68.5 percent and 83 percent respectively. The percentage of misclassified pixels is also less, *i.e.* only three percent for the ‘L’ shape template matching technique.

6.3 Summary

The PCA method is a useful technique for detection of changed pixels. But it is unable to provide explicit information of the changes in the objects of interest.

The 'L' shape template matching method is a useful technique for the change detection of man-made objects such as buildings.

The Performance of the 'L' shape template matching technique is improved when fused Blue band image is used for the feature extraction due to better contrast and as all objects appeared sharper.

The post supervised classification method for the change detection is a useful technique for the preliminary change detection.

Chapter 7

Conclusions

The research examined the use of very high resolution images for buildings extraction and changed detection. Various available techniques for change detection and feature extraction have been reviewed. It has been realized from the literature review that no automated method is available for building extraction and change detection. A new 'L' shape template matching technique has been developed for these tasks.

Traditional change detection methods such as the post supervised classification and the PCA technique have been implemented. The supervised classification method is found unsuitable for change detection of man-made objects such as buildings. The PCA technique is very accurate for change detection but only provides information about the overall changes in the images. The PCA method can not suggest any direct information about the changes in the buildings. Also, the PCA method can not discriminate changes that occur due to missing objects from changes that occur due to the appearance of new objects.

The performance of the 'L' shape template matching method using the fused Blue band is encouraging. The accuracy of the 'L' shape template matching technique has increase by six percent compared to the results obtained from panchromatic image. It is due to the edge detected images obtained using Blue band of synthesized image are sharper and noise free.

An accurate feature extraction is a crucial step for the change detection process. Various image processing techniques have been studied for building extraction. Image processing techniques such as edge detection, image enhancement, corner detector, feature matching, and image segmentation have been used in the developed 'L' shape template matching method for building extraction. The 'L' shape template matching considers only the shape information for the building extraction. This is insufficient for the discrimination of non building objects from building objects. This method is not perfect yet for building extraction. However, this method is certainly useful for the extraction of all linear and curvilinear polygon shape objects.

The recent advancement in the remote sensing community introduced IFSAR (Interferometric Synthetic Aperture Radar) and LIDAR (LIght Detection and Ranging) systems for the development of Digital Surface Model (DSM). Laser (Light Amplification by Stimulated Emission of Radiation) scanning is a fast and precise technique for obtaining elevation information of man-made object such as buildings. By providing elevation information for the feature extraction and change detection of man-made objects, one can discriminate the non building objects from the building objects as elevation gives information about the third dimension of the objects. The use of this elevation information for the buildings will certainly improve the efficiency and the reliability of the building extraction and change detection.

References

- [1] Forstner, W., (1994). A Framework for Low Level Feature Extraction. Computer Vision - ECCV '94, J.O.Eklundh eds, LNCS 802, Springer, vol. II, pp. 383-394.

- [2] Singh, A., (1986). Change Detection in the Tropical Forest Environment of Northeastern India Using Landsat. Remote Sensing and Tropical Land Management. (M.J. Eden and J.T. Parry eds), John Wiley & Son, Chichester, pp. 237-254.

- [3] Howarth, Philip J. and Wickware, Gregory M., (1981). Procedures for Change Detection Using Landsat Digital Data. International Journal of Remote Sensing, vol. 2, pp. 277-291.

- [4] Gautama, S., Goeman, W., (2004). Robust Detection of Road Junctions in VHR Images Using an Improved Ridge Detector. Proceedings ISPRS XXth Congress 2004, Istanbul, vol. XXXV, Part B, pp. 1682-1777.

- [5] Hinz, S., and Baumgartner, A., (2003). Automatic Extraction of Urban Road Networks from Multi-View Aerial Imagery. International Society for Photogrammetry and Remote Sensing, pp. 83-98.

- [6] Schenk, T., (1999). Digital Photogrammetry. TerraScience, Laurelville, Ohio, 236 p.

- [7] Mirmehdi, M., Palmer, P., L., Kittler, J., and Dabis H., (1996). Multi-Pass Feedback Control for Object Recognition. Vision Interface Conference, Toronto, May 1996, pp. 49-56.
- [8] Mirmehdi, M., Palmer, P. L., and Kittler, J., (1998). Optimizing the Complete Image Feature Extraction Chain. Third Asian Conference on Computer Vision, Springer, Verlag, January 1998, vol. 2, pp. 307-314.
- [9] Fischer, G., (1995). Land Resources Assessment: Modeling Food and Agriculture Systems. Elements of Change 1995. Aspen Global Change Institute, Summer Science Session III, Aspen, CO, USA.
- [10] National Research Council (NRC), (2001). Report on Science of Climate Change, National Academy of Sciences, June 2001.
- [11] Wiggins, L., Deuker, K., Ferreira, J., Merry, C., Peng, Z., and Spear, B., (2000) Application Challenges for Geographic Information Science: Implications for Research, Education and Policy for Transportation Planning and Management. Urban and Regional Information Systems Association (URISA) Journal, vol. 12, No. 2, pp. 51-59.
- [12] Jensen, R., Gatrell, J., Boulton, J., and Harper, B. (2004). Using Remote Sensing and Geographic Information Systems to Study Urban Quality of Life and Urban Forest Amenities. Ecology and Society, vol. 9, No. 5, Art. 5.

- [13] Boarnet, Marlon, and Chalermpong, S., (2002). New Highways, House Prices, Urban development: A case study of Toll Roads in Orange County. *Housing Policy Debate*, vol. 12, Issue 3, pp. 575-605.
- [14] Anthony, G. Y., and Xia, Li, (1999). An Entropy Method to Analyze Urban Sprawl in a Rapid Growing Region Using TM Images. *Proceedings of the 20th Asian Conference on Remote Sensing*, 22-25 November 1999. AARS and China Assn for Sci & Tech, pp. 542-547.
- [15] Shettigara, V., Kempinger, S. G., and Aitchison, R., (1995). Semi-Automatic Detection and Extraction of Man-Made Objects in Multispectral Aerial and Satellite Images. *Ascona95*, In: *Automatic Extraction of Man-Made Objects from Aerial and Space Images*, pp. 63-72.
- [16] Opitz, D., (2002a). Feature Extraction Using Spatial Context. *Proceedings of the International ESRI User Conference*, 2002, pp. 813-819.
- [17] Singh, A., (1989). Digital Change Detection Techniques using Remotely-Sensed Data. *Review Article, International Journal of Remote Sensing*, vol. 26, pp. 764-773.
- [18] Phalke, S., and Couloigner, I., (2004). Change Detection of Man made Objects using GIS data & Remotely-Sensed Imagery. *Proceedings of the 24th EARSeL Symposium: New Strategies for European Remote Sensing*, Dubrovnik, Croatia, May 25-27, pp.191-198.

- [19] Oruc, M., Marangoz, A. M., and Buyuksalih, G., (2004). Comparison of Pixel-Based and Object-Oriented Classification Approaches using Landsat-7 ETM Spectral Bands. International Society for Photogrammetry and Remote Sensing XXth Congress, Istanbul, July 2004, commission 4, pp. 1118-1123.
- [20] Warren, A., and Agnew, C., (1988). An Assessment of Desertification and Land Degradation in Arid and Semi-Arid Areas. International Institute for Environment and Development, Drylands Programme, paper no. 2, London: IIED, pp. 103-109.
- [21] Echavarria, F., (1996). Remote Sensing of Forest Fragmentation in the Tropics. IEEE GRS-S Newsletter, June 1996, pp. 6-15.
- [22] Massonnet, D., Rossi, M., Carmona, C., Adragna, F., Peltzer, G., Feigl, K., and Rabaute, T., (1993). The Displacement Field Of The Landers Earthquake Mapped by Radar Interferometry. Nature, vol. 364, no. 6433, 8, 138-142.
- [23] Agouris, P., Gyftakis, S. and Stefanidis, A., (2000). Uncertainty in Image-based Change Detection. Accuracy 2000, July 2000, Amsterdam, The Netherlands, pp. 1-8.
- [24] Agouris, P., Stefanidis, A., Gyftakis, S., and Mountrakis, G., (2002). Differential Object Extraction Methods for Automated GIS Updates. Int. Archives of Photogrammetry and Remote Sensing, vol. 34, Part 4, July 2002, Ottawa, Canada, pp. 781-785.

- [25] Mercier, G., and Derrode, S., (2004). SAR Image Change Detection using Distance between Distributions of Classes. IGARSS 04, Anchorage, Alaska (USA), September 2004, pp. 3872- 3875.
- [26] Girard-ardhuin, Mercier, G., Collard, F. and Garello, R., (2004). Oil Slick Detection by SAR Imagery: Algorithms Comparison. IGARSS 04, Anchorage, Alaska (USA), September 2004, pp. 7803-7807.
- [27] Agouris, P., Mountrakis, G., and Stefanidis, A., (2000). Automated Spatiotemporal Change Detection in Digital Aerial Imagery. Aerosense 2000, SPIE Proceedings, vol. 4054, Orlando, FL, pp. 2-12.
- [28] Huertas, A. and Nevatia, R., (1998). Detecting Changes in Aerial Views of Man-Made Structures. Sixth International Conference on Computer Vision (ICCV'98), January 1998, Bombay, India, pp. 73-80.
- [29] Radke, J. R., Srinivas, A., Omar, A., K., and Badrinath R., (2005). Image Change Detection Algorithms: A Systematic Survey. IEEE Transactions on Image Processing, vol. 14, No. 3. 2005, pp. 294-307.
- [30] Hu, Y., Jong, S., M., and Sluiter, R., (2004). A Modeling-Based Threshold Approach To Derive Change/No Change Information Over Vegetation Area. Geoinformatics 2004, Proc. 12th Int. Conf. on Geoinformatics, June 2004, pp. 647-654.

- [31] Deer, P. J., (1995). Digital Change Detection Techniques: Civilian and Military Applications. Available at: <http://ftpwww.gsfc.nasa.gov/ISSSR-95/digitalc.htm> [Accessed: January 10, 2004].
- [32] Phalke, S., and Couloigner, I., (2005). Change Detection of Linear Man-Made Objects Using Feature Extraction Technique. Proceedings of 3rd International Symposium Remote Sensing and Data Fusion Over Urban Areas (URBAN 2005), Tempe, Arizona, USA, March 14-16, CD-ROM, pp. 5.
- [33] Habib, A., (2003). Remote Sensing Course Notes ENGO 435, Department of Geomatics Engineering, University of Calgary, November 2003.
- [34] Sato, Y., Rastoskuev, R., and Shalina, E., (2005). Remote Sensing Data and Geographic Information Systems. Available at: <http://www.geo.pu.ru/ecobez/edu/books/rsgise/-index.htm>, [Accessed: February 14, 2005].
- [35] Byrne, G. F., Crapper, P. F., and Mayo, K. K., (1981). Monitoring Land-Cover Change by Principal Component Analysis of Multitemporal Landsat Data. Remote Sensing of Environment. vol. 10, 1981 pp. 175-184.
- [36] San, B. T., Sumer, E. O., and Gurcay, B., (2004). Comparison of Band Ratioing and Spectral Indices Methods for Detecting Alunite and Kaolinite Minerals using Aster Data in Biga Region, Turkey. International Society for Photogrammetry and Remote Sensing, XXth Congress, Istanbul, July 2004, Commission 7.

- [37] Hobbs R. J., (1990), Remote Sensing of Spatial and Temporal Dynamics of Vegetation. Remote Sensing of Biosphere Functioning, edited by R.J. Hobbs and H.A. Mooney (New York: Springer Verlag), pp. 203-219.
- [38] Coppin, P., Jonckheere, I., Nackaerts, K., Muys, B. and Lambin, E., (2004). Digital Change Detection Methods in Ecosystem Monitoring: A Review. International Journal of Remote Sensing, vol. 25, pp. 1565-1596.
- [39] Dai, X. and Koharam, S., 1998, The Effects of Image Misregistration on The Accuracy of Remotely Sensed Change Detection, IEEE Transactions on Geoscience and Remote Sensing, vol. 36, pp. 1566-1577.
- [40] Kerekes, J., and Landgrebe, D., (1989). Modeling, Simulation, and Analysis of Optical Remote Sensing Systems. (PhD Thesis) Technical Report TR-EE 89-49, Purdue School of Electrical Engineering, August 1989.
- [41] Trisirisatayawong, I., and Samchimchom, W., (2002). Large Area Change Detection by Differencing Radiometrically-normalized Images. 23rd Asian Conference on Remote Sensing, 2002, Kathmandu, Nepal, Data processing, Algorithm and Modeling session.
- [42] Ha, S., Ahn, B., and Park, Y., (2002). Change Detection of Land-cover from Multi-temporal KOMPSAT-1 EOC Imageries. Korean Journal of Remote Sensing, vol. 18, No.1, 2002, pp.13-23.

- [43] Deer, P.J. and Eklund, P., (2002). Values for the Fuzzy C-Means Classifier in Change Detection for Remote Sensing, Proceedings of the 9th Int. Conf. on Information Processing and Management of Uncertainty (IPMU 2002), IPMU, ESIA - Universite Savoie, 2002, pp.187-194.
- [44] Todd, W. J., (1979). Urban and Regional Land Use Change Detected by Using Landsat Data. Journal of Research by the United States Geological Survey, vol. 5, pp. 527-534.
- [45] Weydahl, D. J., (1991). Change Detection in SAR Images. Proc. of the 1991 Int. Geoscience and Remote Sensing Symposium (IGARSS 91), pp. 1421-1421.
- [46] Cho, Seong-Hoon, (2000). Digital Change Detection by Post-classification Comparison of Multitemporal Remotely-Sensed Data. Journal of the Korean Society of Remote Sensing, vol. 16, No. 4, 2000, pp.367-373.
- [47] Forssén, Per-Erik, (1997). Detection of Man-made Objects in Satellite Images. Department of Electrical Engineering, Masters Thesis, Linkopings University, December 1997.
- [48] Dow, M., Robert and Lewis, B., (2004). An Edge Based Image Segmentation Method. The International Society for Magnetic Resonance in Medicine, Kyoto, Japan, May 2004.
- [49] Wiemker, R., Speck, A., Kulbach, D., Spitzer, H., and Bienlein, J., (1997). Unsupervised Robust Change Detection on Multispectral Imagery using Spectral

and Spatial Features. Third International Airborne Remote Sensing Conference and Exhibition, 7–10 July 1997, Copenhagen, Denmark, vol. I, pp.640-647.

- [50] Wang, F., (1990). Fuzzy Supervised Classification of Remote Sensing Images. IEEE Trans. on Geoscience and Remote Sensing, vol. 28, 1990, pp. 194-201.
- [51] Zhang, Q., and Couloigner, I., (2004). A Framework for Road Change Detection and Map Updating. The International Archives of the Photogrammetry, Remote Sensing and Spatial Information Sciences, vol. XXXV, Part B2, Istanbul, Turkey, July 12-23, pp. 729-734.
- [52] Agouris, P., Stefanidis, A., and Gyftakis, S., (2001). Differential Snakes for Change Detection in Road Segments. Photogrammetric Engineering and Remote Sensing vol. 67, No. 12, December 2001, pp. 1391–1399.
- [53] Japan Association of Remote Sensing (JARS), (1996). Remote Sensing. Available at: <http://www.profc.udec.cl/~gabriel/tutoriales/rsnote/contents.htm>, [Accessed: February 20, 2004].
- [54] Opitz, D. (2002b). Hierarchical Feature Extraction: Removing the Clutter. Proceedings of the International ESRI User Conference, 2002, pp. 924-930.
- [55] Schyns, P., Goldstone, R., and Thibaut, Jean-Pierre, (1998). The Development of Features in Object Concepts. Behavioral and Brain Sciences, 1998, vol. 21, pp. 1-17.

- [56] Ohlhof, T., Emge, T., Reinhardt, W., Leukert, K., Heipke, C., and Pakzad, K., (2000). Generation and Update of VMap Data using Satellite and Airborne Imagery. In: International Archives of Photogrammetry and Remote Sensing (IAPRS), Vol. XXXIII, Part B4, pp. 762-768.
- [57] Hoàng, Q. V., Phan, T., Andro, O., and Mai, T., (2004). Fusion of Multiresolution and Multisensor Imagery. Journal of Geology Series, No 22, Art 14.
- [58] Meenakshisundaram V., and Couloigner, I. (2004). Image Fusion of IKONOS PAN and Multi-spectral images for Classification of Urban Environment. Proceedings of the 24th EARSeL Symposium: New Strategies for European Remote Sensing, Dubrovnik, Croatia, May 25-27, pp.335-342.
- [59] Lillesand, T., M., and Kiefer, R., W., (2000). Remote Sensing and Image Interpretation. 5th ed. John Wiley & Sons, Inc., 2000.
- [60] Wald, Lucien, (2002). Data Fusion: Definitions and Architectures. Les Presses de l'Ecole des Mines, Paris, 2002.
- [61] Harris, C. and Stephens, M., (1988). A Combined Corner and Edge Detector. In: 4th Alvey Vision Conference, 1988, pp. 147-151.
- [62] Chavez, P.S. Jr., Sides, S.C. and Anderson, J.A., (1991). Comparison of three different methods to merge multiresolution and multispectral data: Landsat TM

and SPOT panchromatic, *Photogrammetric Engineering and Remote Sensing*, vol. 57, No.3, pp.295-303.

- [63] Sobel, I., (1990). An isotropic 3x3 image gradient operator. In H. Freeman, editor, *Machine Vision for Three-Dimensional Scenes*, Academic Press, 1990, pp. 376-379.
- [64] Canny, J. F., (1983). *Finding Edges and Lines in Images*. Master's thesis, MIT, Cambridge, USA, 1983.
- [65] Canny, J. F., (1986). A Computational Approach to Edge Detection. *IEEE Trans. on Pattern Analysis and Machine Intelligence*, November 1986, vol. 8, No. 6, pp. 679-698.
- [66] Mortenson, E., and Barrett, W. A., (1998). Interactive Segmentation with Intelligent Scissors. *Graphical Models and Image Processing*, vol. 60, No. 5, pp 349-384.
- [67] Prewitt, J. M. S., (1970). *Object Enhancement and Extraction*. *Picture Processing and Psychopictorics*, (Lipkin and Rosenfeld Eds.), Academic Press, New York. 1970.
- [68] Gonzalez, R. C. and Woods, R. E., (2001). *Digital Image Processing*, 2nd Ed., Prentice Hall, Upper Saddle River, NJ.

- [69] Quddus, A., Cheikh, F. A., and Gabbouj, M., (1999). Content-Based Object Retrieval using Maximum Curvature Points in Contour Images. Proc. SPIE, vol. 3972, pp. 98-105.
- [70] Forstner, W. and Gulch E., (1987). A Fast Operator for Detection and Precise Location of Distinct Points, Corners and Centers of Circular Features. In: ISPRS Intercommission Workshop, Interlaken, pp. 149-155.
- [71] Moravec, H., (1979). Visual Mapping by a Robot Rover. Proc. of the 6th International Joint Conference on Artificial Intelligence, Tokyo, Japan, pp.598-600.
- [72] Montesinos, P., Gouet, V., and Deriche, R., (1998). Differential Invariants for Color Images. ICPR, 14th 1998, vol. 01, No. 1, pp. 838.
- [73] Smith, S., (1992). Feature Based Image Sequence Understanding. D.Phil. thesis, Robotics Research Group, Department of Engineering Science, Oxford University, 1992.
- [74] Smith, S. and Brady J. M., (1997). SUSAN—A New Approach to Low Level Image Processing. International Journal of Computer Vision, May 1997, vol. 23, No. 1, pp. 45-78.
- [75] Pilon, P.G., Howarth, P.J., Bullock, R.A. and Adeniyi, P.O., (1988). An Enhanced Classification Approach to Changes in Semi-Arid Environments. Photogrammetric Engineering and Remote Sensing, vol. 54, pp. 1709-1716.

- [76] Wang, H., and Ellis, E., C., (2005). Spatial Accuracy of Orthorectified IKONOS Imagery and Historical Aerial Photographs across Five Sites in China. *International Journal of Remote Sensing*, May 2005, vol. 26, No. 9, pp. 1893-1911.
- [77] Richards J. A., (1993). *Remote Sensing Digital Image Analysis: An Introduction*. (2nd ed) Springer, Heidelberg, New York, 1993.
- [78] Guennadi, G., and Yerach, Doytsher, (2003). Geographic Information System Data for Supporting Feature Extraction from High-Resolution Aerial and Satellite Images. *Journal of Surveying Engineering*, November 2003, vol. 129, Issue 4, pp. 158-164.
- [79] Horne, J., (2003). A Tasseled Cap Transformation for Ikonos Images. *ASPRS 2003 Annual Conference Proceedings*, May 2003, Anchorage, Alaska, pp. 34-43.